

We thank the anonymous reviewers for their helpful comments. These comments helped to substantially improve the manuscript. As a consequence of the referee reports we decided to do a reanalysis of the data to address the main concerns of the referees, namely the relatively large mass absorption cross section of the Fullerene soot as well as the absorption cross section and mass size distribution of the snow samples. Further, the referees are concerned about the language and structure of the manuscript. In conjunction with the results of the reanalysis the manuscript text was almost completely re-written. Both, the reanalysis and the writing were mostly done by Martin Schnaiter, and, therefore, we decided to switch the lead author role to him. This of course with consent of Claudia Linke and all co-authors.

In the following we give detailed answers to the individual reviewer comments in blue.

Answer to Referee Comment 1 (Reviewer #3)

Manuscript: Specifying light absorbing properties of aerosol particles in fresh snow samples, collected at the Environmental Research Station Schneefernerhaus (UFS), Zugspitze (Linke et al.)

It is often regarded that the polar regions are the “canary in the coal mine” regarding this region’s sensitivity to changes in radiative forcing. This sensitivity derives, in part, from the very high surface albedos that typify these regions. However, despite the recognized importance of this subject, our quantitative understanding of the radiative contribution by light absorbing aerosols - be it atmospheric or surface-deposited particles - in these regions - and on snow/ice - is still very low. Therefore, more research is indeed needed to improve our understanding of this subject and to reduce the associated uncertainty. To this end, the manuscript by Linke and co-workers undertake an investigation of light absorbing properties of aerosols deposited on snow near the Environmental Research Station Schneefernerhaus with the goal to better quantify the aerosol types (classes) of light absorbing aerosols present in this region. To derive the optical properties, these researchers combine aerosol light absorption measured by a photoacoustic spectrometer with refractory black carbon (rBC) mass loading measurements reported by a single particle soot photometer (SP2) on re-aerosolized snow samples. The insights and data that can be gleaned from a study such as this is of value and should, eventually, be published. But in its current state, the manuscript is not ready and thus is not recommended for publication at this time.

One of the biggest issues this reviewer has centers on how these researchers are combining their light absorption and rBC mass measurements. In the atmospheric aerosol community, we take these two datasets and derive the mass absorption cross- section (MAC; m²/g). This property enables researchers to say something about the mixing state of the rBC particles as well as something about aerosol type (e.g., the presence/absence of light absorbing organic material/particles (e.g., brown carbon or BrC and dust). However, despite the ubiquity of this methodology in our community, the authors, instead, advocate using a methodology that compares the SP2-derived mass with what they term as a “fullerene soot equivalent mass” derived from the photo acoustic spectrometer. In order to use a “fullerene equivalent mass” derived from the light absorption measurements the researchers must assume that the MAC is constant - the literature is populated with many studies that show that the MAC is not constant. For example, at 550 nm, the black carbon MAC for fresh (uncoated) soot is ~ 7.5 m²/g while for thickly-coated black carbon particles this value could be 12-14 m²/g at this wavelength, thus representing a factor of 2x change. How do the authors account for the potential changes in the MAC brought about by changes in the rBC mixing state? Why not simply derive a MAC and utilize the variability in this value to infer something about the light absorbing particles deposited on the snow? The authors provide no justification as to why their methodology is preferred. If the

authors feel strongly that this methodology offers an advantage not available with a MAC-based methodology, then they need to present that argument. Further, any sources of error in the interpretation of the data using this methodology is not addressed and needs to be.

The referee can be sure that the authors know the importance and the ubiquity of the MAC in the atmospheric aerosol community as they published important contribution to this field in the past (e.g. Schnaiter et al., 2003; Schnaiter et al., 2005; Schnaiter et al., 2006). The authors used the optical equivalent BC mass here because it was used in one of the most comprehensive studies on light absorbing impurities in Arctic snow by Doherty et al. (2010). Also, the authors are aware of the fact that the MAC is not constant in the atmosphere and the MAC of thickly coated soot can be enhanced by a factor of two, as they provided the first experimental proof of this effect already in 2005 (Schnaiter et al., 2005). However, the authors agree that the presentation of the absorption measurements is insufficient in the manuscript. Therefore, we did a thorough reanalysis of the snow samples following the following strategy that also includes a MAC analysis of the data:

1. The snow mass specific absorption cross section σ_{abs} [m^2/mL] was deduced from the absorption coefficient b_{abs} [m^{-1}] using the nebulizer flow settings and the nebulizing efficiency (Eq. 1 of the revised manuscript):

$$\sigma_{abs} = 10^{-3} \cdot b_{abs} \cdot R_{neb} / R_{pp} \cdot \varepsilon_{neb}^{-1}$$

2. This snow mass specific absorption cross section is plotted as a function of the refractory BC mass concentrations in a new figure (Fig. 10 of the revised manuscript). Linear regression fits to the data then give the BC mass specific MAC of the snow samples. We found MAC values that are up to a factor of two larger than the MAC of Fullerene soot. A table is added to the manuscript contrasting the mass and optical properties (including the MAC) of Fullerene soot with those of the snow samples.
3. To be comparable with other studies (e.g. Doherty et al., 2010), we calculated the equivalent BC mass concentration c_{BC}^{equiv} , i.e. the amount of BC that would need to be present in the snow to account for the measured absorption, from σ_{abs} using the MAC of Fullerene soot (Equation 2 of the revised manuscript):

$$c_{BC}^{equiv} = \sigma_{abs} / \text{MAC}_{FS}$$

4. We plotted c_{BC}^{equiv} as a function of the refractory BC mass concentration in a new figure (Fig. 11 of the revised manuscript) and found a good correlation of both concentrations but with correlation coefficients of 2.0, 1.9, and 1.4 for 405, 532, and 658 nm, respectively (note that c_{BC}^{equiv} is a function of the wavelength). We conclude from this that there is additional non-BC light absorbing mass in the snow, which is correlated with the BC mass and which has a strong wavelength dependence between the green and the red part of the visible spectrum. This already indicates mineral dust and organic (brown) carbon as possible carriers of this additional absorption.
5. We calculated the snow mass specific absorption cross section of the non-BC particles, σ_{abs}^{nonBC} (Equation 3 in the revised manuscript):

$$\sigma_{abs}^{nonBC} = \sigma_{abs} - c_{BC}^{SP2} \cdot \text{MAC}_{FS} \cdot 10^{-9}$$

We added a figure (Fig. 12 in the revised manuscript) that shows the statistical analysis of the σ_{abs}^{nonBC} for the snow samples and that compares this non-BC spectral

behavior with laboratory data for Saharan dust and organic (brown) carbon (see answer to the previous comment).

Continuing, this reviewer is very concerned about the reported MAC values for the fullerene standard. Fullerene soot should be uncoated and thus should exhibit a MAC that is characteristic of an uncoated black carbon particle, namely a MAC $\sim 7.5 \text{ m}^2/\text{g}$ at 550 nm. Yet, at 532 nm, the authors report a MAC of $10.6 (+/- 2.8) \text{ m}^2/\text{g}$ - a value that is $\sim 40\%$ larger than the canonical value for denuded soot, and 65% larger than the fullerene MAC reported by Zhou ($6.4 \text{ m}^2/\text{g}$) - work cited by the authors. Additionally, it is also at odds with the recently published value by Zangmeister $6.1 \text{ m}^2/\text{g}$ at 550 nm (Carbon (2018), doi: 10.1016/j.carbon.2018.04.057). The disagreement is quite critical as it will have bearing on interpretation of data collected on the snow samples. While the authors are correct that the BC MAC is dependent on particle size, using the argument that the differences between their higher values and that reported by others as being due to differences in the sample size distribution studied is not correct. Using a refractive index of $1.95-0.79i$ (Bond & Bergstrom (2006); Aero. Sci. Tech. 40:1, 27- 67) a straight forward Mie calculation reveals that the maximum MAC calculated for a BC is $\sim 7.9 \text{ m}^2/\text{g}$ for a BC diameter of 150 nm and that the MAC only goes down with either increasing or decreasing particle size. Therefore another explanation is needed. Three potential explanations submitted here are: (i) either the fullerene soot is coated and the derived MACs reflect a lensing-enhanced value or (ii) there are some non- BC, light absorbing aerosols present in the sample, or (iii) the number concentrations used during the fullerene soot calibration are high enough that particle coincidence is occurring that the post-processing of the SP2 data does not correct for. This latter possibility is brought up because particle-resolved measurements, like the SP2, can easily find themselves in the particle-coincidence regime. Such an undercounting of the actual fullerene mass would bring the reported MACs down and thus reconcile their MAC values with others. The authors are encouraged to insure that the SP2 is not operating in this regime.

We do not agree with the Referee that the MAC of uncoated BC is canonical with a constant value of $7.5 \text{ m}^2/\text{g}$. Only because something is continuously referenced does not necessarily mean that it is correct. A constant MAC would mean that refractive index of the material is constant. From a solid-state physical perspective this is highly uncertain in case of carbonaceous material with its variable electronic band structures. Already pure carbon can exist in five different allotropes including graphite and diamond – one is black the other transparent – so obviously completely different refractive indices. Adding now the morphological variability of fractal soot particles to the discussion with a wealth of different monomer sizes, monomer nonsphericity (irregularity), necking, and overlapping (even on a single particle) that all have an influence on the particle absorption cross section, it is conclusive to the authors that the absorption cross section of this material cannot be constant but depends on its formation conditions. Further, the MAC is calculated from the absorption cross section and the particle mass. Particle mass is measured in different ways – sometimes as a total mass (including non-refractory compounds as in the DMA-APM method), sometimes as a refractory mass only (as with the SP2). So, there comes an uncertainty also from this side into the MAC. It is correct that Fullerene soot was identified as a good standard for atmospheric BC in terms of the SP2 mass sensitivity (although with a variation of 15% from batch to batch). But does that mean that this is also the case for its spectral absorption properties given the variability in the electronic and microphysical structures discussed above? With all this, the authors do not see any reason why a laboratory to laboratory difference in published MAC values of 30-40% shouldn't be within the variability range of the material itself, the size differences and the mass measurement methods used in the different studies.

The authors took care that the SP2 wasn't operated under aerosol concentrations that would result in coincidence errors. However, it turned out that due to the upper cut size of the SP2 (560 nm), we missed about 10% of the Fullerene particle mass. In the reanalysis we therefore applied lognormal fits to the measured BC mass size distributions to account for this mass outside the SP2 sizing range (see Fig. 6 of the revised manuscript). With this

correction the MAC of FS is reduced to 9.5 ± 2.2 m²/g (532 nm). Further, to be comparable with the Zangmeister et al. (2018) study who measured the MAC on size-selected FS particles, we also measured the MAC of size selected Fullerene soot particles in a separate study by adding a DMA behind the Marin-5. We found a MAC of 8.6 m²/g for the same mobility-equivalent diameter (350 nm) as used in the Zangmeister et al. study. This is still 40% larger than the 6.1 m²/g of Zangmeister et al., but given the fact that (i) a APM/DMA was used for the mass measurement in their study and (ii) they used a different batch of Fullerene soot, this difference is within the range of variability that can be expected in such a comparison.

The whole Sect. 4 was rewritten to make the discussion of the Fullerene soot MAC clearer:

"Simultaneously to the BC mass concentration measurements with the SP2, the absorption coefficients b_{abs} of the Fullerene soot suspensions were measured for the three PAAS-3λ wavelengths. Both measurements together enable the determination of the mass specific absorption cross section $MAC_{FS} = b_{abs}/c_{BC}^{SP2}$ of airborne Fullerene soot at 405, 532, and 658 nm. In **Error! Reference source not found.**, the absorption coefficients b_{abs} are plotted against the SP2-derived BC mass concentrations c_{BC}^{SP2} of the Fullerene soot suspension standards. Linear regression fits of the data result in MAC_{FS} values of 10.5 ± 3.2 m²/g, 9.5 ± 2.2 m²/g, and 8.6 ± 3.3 m²/g for 405, 532, and 658 nm, respectively. The MAC_{FS} at 532 nm is comparable to the value of 8.84 m²/g given by Schwarz et al. (2012) for Fullerene soot (lot #F12S011) deduced from ISSW measurements, but is significantly higher than the 6.1 ± 0.4 m²/g (mean $\pm 2\sigma$) measured recently by photoacoustic absorption spectroscopy for size selected Fullerene soot particles by Zangmeister et al. (2018). They used a combination of a differential mobility analyzer (DMA) and an aerosol particle mass analyzer (APM) to select Fullerene soot particles within a narrow mass range from aerosol generated by an atomizer. Their MAC_{FS} of 6.1 m²/g, which is given for a wavelength of 550 nm, a mobility-equivalent diameter of 350 nm, and for a particle mass of $16.6 \cdot 10^{-15}$ g, corresponds to a volume-equivalent diameter of 264 nm using a density of 1.72 g/cm³ of Fullerene soot (Kondo et al., 2011). Although, this diameter is not very different to the MMD of 228 nm of the Fullerene soot suspensions used here, part of the observed discrepancy can be attributed to the different sizes as the MAC is strongly depending on the particle diameter for particles larger than about 200 nm (e.g. Moosmüller et al., 2009). To be comparable, we measured the MAC_{FS} of size selected Fullerene soot particles in a separate study by adding a DMA behind the Marin-5 in the setup shown in **Error! Reference source not found.**. A MAC_{FS} of 8.6 m²/g was measured for the mobility-equivalent diameter of 350 nm, which is still ~40% larger than the MAC_{FS} given by Zangmeister et al. (2018) for the same diameter. However, they used an APM to measure the BC mass, while a SP2 was used here to deduce the refractory BC mass. According to Laborde et al. (2012a), the Fullerene soot product shows a variability from batch to batch, which results in a SP2 calibration uncertainty of up to 15% (actually only two batches were compared; lot #F12S011 and lot #L18U002). They explained the differences in the SP2 response (i.e. the calibration curves) by a substantial non-refractory coating in case of the L18U002 batch that could be identified by thermodenudation of the samples. Assuming that lot #W08A039 used in Zangmeister et al. (2018) has a similar coating, this would increase the APM mass measurement by about 15% compared to the SP2-derived BC mass of lot # F12S011 used in the present study. This in turn would increase the MAC_{FS} from 6.1 m²/g reported by Zangmeister et al. (2018) to about 7 m²/g when using only the refractory BC mass fraction in the calculation of the MAC_{FS} . This assumption reduces the discrepancy between the two MAC_{FS} values to 35%, which is within the uncertainty range of ± 2.2 m²/g for our 532 nm value. It is further conceivable that different batches of the Fullerene soot material have different electronic band structure (i.e. refractive index) and/or fractal aggregate structures that both change the absorption cross section of the particles at a constant particle mass (e.g. Liu et al., 2019; Zangmeister et al., 2018). **Error! Reference source not found.** shows an electron micrograph of a typical Fullerene soot aggregate sampled from the dry aerosol output of the Marin-5 nebulizer. Thus, the Fullerene soot particles do not have a simple fractal aggregate structure, but are

rather complex-structured with polydisperse monomer sizes, monomer nonsphericity (irregularity), necking, and overlapping, which all have a significant impact on the optical particle properties (including the absorption cross section) compared to the idealized fractal aggregate (Teng et al., 2019). Since these microphysical details of the soot particles are very sensitive to the actual formation and subsequent treatment conditions (Gorelik et al., 2002), it is conclusive that the MAC_{FS} has an even higher variability between different Fullerene soot batches compared to what is expected from the SP2 mass sensitivity only.

The wavelength dependence of the aerosol light absorption, expressed by the so-called absorption Angström exponent (AAE), was determined to be 0.46 ± 0.07 for the used Fullerene soot suspensions by analysing the b_{abs} data for the 405 and 658 nm wavelengths. This AAE is close to the ~ 0.6 reported by Baumgardner et al. (2012) for Fullerene soot derived from multiwavelength PSAP and Aethalometer measurements and it is within the range of the 0.54 ± 0.06 determined by Zhou et al. (2017) from ISSW spectrometer measurements on Fullerene soot filter samples in the 450 nm to 750 nm spectral range. However, it is significantly lower than the 0.92 ± 0.05 given by Zangmeister et al. (2018) for Fullerene soot lot #W08A039. Here again, we have to take into account that Zangmeister et al. (2018) analyzed size segregated absorption spectra and their AAE is given for a mobility-equivalent diameter of 350 nm. Analyzing our size segregated measurements gives an AAE of 0.82 ± 0.02 for the same mobility-equivalent diameter, which is close but smaller than the Zangmeister et al. value, further supporting the above assumption that there is a difference in the chemical as well as physical (including optical) properties between different batches of the Fullerene soot product.“

While on this subject, what were the re-aerosolized number concentrations in the snow samples studied? On lines 243-244, the authors state that “...Marin-5 nebulizer was then fixed at a rate of 0.32 mL min^{-1} , which guarantees a high enough particle mass concentration for the photo acoustic measurement. Depending upon the mass concentration and mode size of the particles, this could hint at co-incidence issues with the SP2.

The concentrations behind the Marin-5 were always low enough ($< 1000 \text{ #/cc}$) to avoid any coincidence issues.

Other specific issues:

Do the authors worry about the loss of water soluble BrC during sample preparation that might not be reflected when re-aerosolizing their snow samples?

We do not have any information on potential soluble BrC mass loss.

Line 167: What were the PSL diameters used? While the incandescence channel of the SP2 is sensitive enough to detect $< 100 \text{ nm}$ rBC particles, the scattering channel is typically limited to optical diameters $> 200 \text{ nm}$. What is the particle number loading in the instruments (see reference to coincidence above)

The characterisation of the particle number efficiency of the nebulizer and the daily performance control was performed with monodisperse polystyrene latex (PSL) particles (Postnova Analytics GmbH, Landsberg am Lech, Germany) with nominal diameters of $240 \pm 5 \text{ nm}$ and $304 \pm 5 \text{ nm}$. The particle number concentration within these suspensions is about $3 \cdot 10^8 \text{ 1/mL}$. A diluted PSL standard suspension sample was prepared daily by pipetting 1 mL suspension into a 100 mL graduated flask filled with Nanopure water. This results in a concentration of typically a few hundred particles per cc at the output of the Marin-5.

Line 291-293: The authors report and discuss the “enhancement” factor of the soot- equivalent mass derived from the photoacoustic spectrometer with decreasing wave- length (1.65, 2.28, and 2.38 at 658 nm, 532, 405 nm, respectively) and conclude that this suggests these samples

might contain mineral dust or BrC. The data might be able to say something more concrete. While the authors should conduct a more thorough literature search, mineral dust tends to absorb more in the red than the blue, whereas BrC exhibits the opposite wavelength dependence. The wavelength dependence of light absorption observed in the present study suggests that the non-rBC absorbing species is BrC. Also, it should be noted that BrC can exhibit absorption at the red wavelengths, though, again, the wavelength dependence favors more absorption in the blue (e.g., tar balls: Hoffer, et al., 2017. Brown carbon absorption in the red and near infrared spectral region. *Atmos. Meas. Tech.* 10(6): 2353–59).

Although we cannot directly measure the dust concentrations in the snow samples, we can draw some conclusion by analyzing the spectral signature of the snow mass specific absorption cross section of the non-BC particles, i.e. after subtraction the spectral cross section that is expected from the SP2 mass data using the MAC of Fullerene soot (Equation 3 of the revised manuscript; see Point 5 above). We added a figure (Fig. 12 in the revised manuscript) that shows a comparison of the non-BC spectral absorption cross section with laboratory absorption data for Saharan dust particles. Thus, Saharan dust is a good candidate to explain the observed non-BC light absorption in the snow samples. We did the same comparison with laboratory data of OC, which reveals that OC could also explain the observed non-BC absorption - not only in terms of wavelength dependence but also in terms of variability.

The whole paragraph on the analysis of the spectral absorption analysis has been rewritten to make our argumentation of a significant influence of non-BC particles on the light absorption in snow clearer.

line 349: "The term brown carbon is not clearly defined or characterized." This is very misleading. Simply put, brown carbon, BrC, is organic aerosol that absorbs light. While the chemical composition for any given BrC aerosol may vary, as long as the organic aerosol absorbs light it is cataloged as BrC. Please reword this sentence.

Paragraph rephrased to:

"The term "brown carbon" is mainly related to a strong wavelength dependence of the visible light absorption observed in these materials. From a chemical perspective, BrC can generally be divided into humic-like substances (HULIS) and tar balls (Wu et al., 2016). HULIS can be characterised mainly as a mixture of macromolecular organic compounds with various functional groups and are expected e.g. in oxidation processes of biogenic precursors (Wu et al., 2016). Tar balls are emitted from biomass burning and are of spherical, amorphous structure and are typically not aggregated. Moreover, light absorbing organic material and HULIS can be formed from the water-soluble fraction of biomass burning aerosol compounds, and is therefore suggested as an atmospheric process for the formation of light absorbing BrC in cloud droplets (Hoffer et al., 2004). Further examination of snow samples from different locations as well as systematic investigations on the optical behaviour of biogenic particulate matter is therefore necessary to evaluate the influence of biogenic (including biological), BrC and mineral dust on the aerosol absorption properties in the visible spectral range."

Please provide plot of fullerene standard size distribution.

Added (Fig. 6 of the revised paper).

Editorial comments

There is no reason to put quotes around the word fullerene.

Agreed and changed.

Line 67: "Most Himalayan glaciers as glaciers elsewhere have retreated..." Please insert comma after first occurrence of the word "glaciers" and after "elsewhere".

Introduction has been completely reworded.

Line 311: "To get a general idea of the nature of the components that are solved and dissolved within the snow samples ionic chromatography ..." the word "solved" does not seem right here. Please check and correct as necessary.

Reworded to:

"To further examine the nature of the particulate components that are deposited in the snow samples ion chromatography (IC) ... "

Answer to Referee Comment 2 (Reviewer #2)

We thank the anonymous reviewer for the helpful comments. These comments helped to substantially improve the manuscript. Below we give detailed answers to the individual reviewer comments in blue.

Referee Comments for: "Specifying light absorbing properties of aerosol particles in fresh snow samples, collected at the Environmental Research Station Schneefernerhaus (UFS), Zugspitze"

General Comments:

This manuscript presents a novel method for concurrently measuring the rBC mass concentration and total aerosol absorption in snow. The authors find a discrepancy between the SP2-measured rBC concentration and a calculation of rBC concentration that is based on total aerosol absorption and a fullerene-standard's MAC. The former being smaller than the latter, the authors conclude the likely presence of non-rBC absorbing aerosols in the snow. WIBS measurements indicate that the larger of these non-rBC aerosol are predominantly of biological origin. These results are both interesting and important, as the presence and properties of light-absorbing aerosols in snow and their impact on snow/ice melt is not presently well understood.

Overall, the methodology of the measurements seems sound, and the text contains all of the necessary information to understand the experiment. I have four main concerns, three of which are science-related, and one regarding the writing. These can be found in the 'Specific Comments' below. I believe that once these things are appropriately addressed, the manuscript deserves publication in ACP.

Specific Comments:

My first concern is that this study's calculated MAC for fullerene soot is quite high compared to other literature, which typically put it around 7 m²/g or so. The authors acknowledge this, but I don't feel they explore (at least in the text) the underlying cause sufficiently. As this is at least somewhat dependent on the size of the fullerene particles, I suggest that the fullerene standard's size distributions be added to Figure 8.

First, we added a figure (Fig. 6 in the revised manuscript) that shows the refractory BC mass size distributions of our Fullerene suspension standards. Second, these size distributions were fitted by lognormal distributions to get the missed mass beyond the upper size limit of our SP2. The analysis of the Fullerene MAC was then redone with the corrected BC mass, resulting in lower MAC values of 10.5 ± 3.2 , 9.5 ± 2.2 , and 8.6 ± 3.3 m²/g for 405, 532, and 658 nm, respectively. Third, we completely rephrased Sect. 4 in the revised manuscript that now includes a comparison with published MAC of Fullerene soot and a discussion of potential reasons why our values are larger. This discussion includes the influence of different particle size distributions, different methods to deduce the particle mass, differences in using different Fullerene soot batches as well as the in general higher sensitivity of light absorption to BC electronic band structures and fractal aggregate morphologies compared to the incandescence mass detection.

Second, the authors don't estimate the percentage of rBC in snow that is above the detection limit of the SP2. Again, the authors acknowledge the issue, beginning on line 278, by stating that the SP2 only detects rBC up to 500 nm VED, but then rather simply declare the mass beyond this as small. The size distribution in Figure 8 indicates that there is still non-negligible mass above 500nm, and exactly how much can easily be estimated using a lognormal fit to the distributions. I attempted to estimate this by extracting data from the plot (see my attached figure), doing my own fit, and calculating percentage of area under the curve that is above 500nm. . . I get about 10%. Furthermore, it's highly doubtful that the SP2 is detecting with 100% efficiency below 60-70nm or so. This probably has a smaller effect on the total rBC mass, but including that data in a lognormal fit could skew the fit

result. If I do the same fit, but only use the size distribution data between 70 – 500 nm, I come up with ~13% of the mass above the detection limit. Of course, this is just an ‘eyeball’ estimate on my part, and may be off by a bit. I suggest the authors do a more careful check and add the details to the text.

As suggested by the reviewer, we performed a more careful analysis of the refractory BC size distributions of the snow samples. First, we divided the samples in the periods Nov-Jan, Feb-Mar, and Apr-May to check any seasonality in the data. Second, we performed lognormal fits to the data between 70 and 500 nm as suggested by the reviewer and found a mass fraction of 10 to 20% that is beyond the upper size limit of our SP2. Third, we compared our size distributions with the average SP2 size distribution measured for five snow samples collected after three snowfall events in the semi-rural and rural surroundings of Denver, CO, USA by Schwarz et al. (2013). Our size distributions agree very well with the Schwarz et al. distribution, who measured the distribution up to a size of $2 \mu\text{m}$ (see Fig. 9 of the revised manuscript). Due to this good agreement and the fact that the size distributions are skewed with a shoulder towards larger sizes, we decided to use the 28% given by Schwarz et al. for the mass fraction $> 600 \text{ nm}$ to correct our snow sample SP2 data.

Ideally, the gain on one of the SP2’s incandescent channels should have been set so as to extend the detection limit. The fact that it wasn’t does not necessarily damage the story the paper is telling, in my opinion. . .but nevertheless, more care should be given to estimating the effects of this. Ultimately, the SP2-determined rBC concentrations presented in the manuscript are more appropriately viewed as low-bounds until corrected for the undetected rBC mass. Note also that accounting for the undetected rBC would bring the SP2-determined concentration and the PAAS-3L calculated- concentration into better agreement.

See answer to the previous comment. With a correction factor of 1.39 that we applied to the SP2 data in the reanalysis (i.e. accounting for a fraction of 28% missed mass), we are rather on the upper limit for this correction. In this way, however, we are confident that the main conclusion of our paper namely that there is a significant contribution of non-BC particles to light absorption in fresh snow is solid.

Third, on Line 192: The concentration of the PSL standard is higher than I’m comfortable using for my own Marin-5+SP2 setup. . .I wonder if there was any evidence of multiple PSL particles existing within a single SP2 trigger? This could affect the efficiency calculation. It’s easy enough to look through the raw SP2 data and confirm that this isn’t a common occurrence for their data. I’m not claiming that I expect that there is a major issue, but simply that it should be looked for when using concentrations that high. Further, the authors do not include the size of the PSLs. . .this should be stated.

We think that our PSL concentrations are not too high. The manufacturer suspension has a concentration of $3 \cdot 10^8 \text{ #/mL}$, which is further diluted by a factor of 100 before it is used in the characterization of the Marin-5. With the Marin-5 flow settings and the known dispersion efficiency of 36% we end up with a few hundred particles per cc at the Marin-5 output, which is definitely not an issue for the SP2 measurement in terms of coincidence.

Finally, in general, the writing needs some ‘smoothing’, as certain word choices and sentence structures don’t flow as well as they could. I would recommend a careful proofreading.

The manuscript has been thoroughly restructured and reworded.

The technical corrections listed below are addressed in the revised manuscript.

Technical Corrections:

General comment: I see no need to continually put ‘fullerene’ in parenthesis Line 56: extend -> extent

Line 64: I don’t like the phrasing “should be” in this circumstance. I’d suggest something like “The authors determined albedo values of only 0.5-0.7 for the ultraviolet and visible range, substantially lower than the 0.97-0.99 that is typical for clean snow [include a citation]”

Line 67: "Most Himalayan glaciers as glaciers. . ." - > Should this be "Most Himalayan glaciers and glaciers"?

Line 74: smooth wording of sentence beginning "In the last decade. . ."

Line 96: analyses -> analyzes

Line 118: remove word 'used'

Line 207: the authors use the word 'daily' twice in quick succession. Again, smooth the writing here

Line 221: depending -> dependent

Line 225: the phrase "it turned out" is too colloquial for a scientific paper

Line 268: remove the word 'used'

Line 282: please add the word 'these' to specify that this statement isn't generally true (for instance, in the case of snow that has experienced freeze/thaw), i.e. "Thus, the majority of the rBC particles in these fresh snow samples have. . ."

Line 322: The use of the word "therefore" is not appropriate here. Recommend reword- ing.

Answer to Referee Comment 3 (Reviewer #1)

We thank the anonymous reviewer for the helpful comments. These comments helped to substantially improve the manuscript. Below we give detailed answers to the individual reviewer comments in blue.

Review of Linke et al. 'Specifying light absorbing properties of aerosol particles in fresh snow samples, collected at the Environmental Research Station Schneefernerhaus (UFS), Zugspitze.'

General comments:

This paper present results from snow samples analyzed for their aerosols content over one winter season. The authors are using an array of different instrumentation, making this an interesting study that is most certainly within the scope of ACP. In light of the instrumentation used in this study, it appears that the authors have not presented the full potential of the data that should be at hand in the current version of the manuscript. For example: absorption measurements coupled with the BC mass content have been carried out, enabling the authors to present direct MAC values for the particulates in the snow (which could then be used for comparison and additional data in the manuscript). Another issue that should be addressed more thoroughly in the manuscript, is the fact that it seems as there is only the one sample (from March 10th) where the additional analyzes are performed, and from this one sample conclusions about all of the snow samples are drawn. Please see further comments below on these topics, as well as some other questions and recommendations that should be addressed. Lastly, the manuscript's language should be checked and re-evaluated for a better read. Although I'm not a native English speaker myself, I do believe the manuscript would benefit from such a procedure. Some mistakes have been highlighted in the technical corrections below, but I'm sure there are mistakes that I have missed, and so make sure to check the whole manuscript. On the whole, this work would be a welcomed addition to the literature after it has been majorly revised.

We agree with the reviewer that we have not presented the full potential of our measurements and data. That's why we have made efforts to include a more thorough analysis of the data, resulting in additional discussions (which includes now also comparisons with literature data) of (a) the MAC of "Fullerene" soot, (b) the MAC of the snow samples, and (c) the spectral absorption of the non-BC particles in the snow. While the ESEM and fluorescence analysis of further snow samples is certainly something that would strengthen our conclusions, we refrained from doing them simply because these analyses (especially with the ESEM) are very time consuming and expensive, which we couldn't invest at this time for this project. Finally, the manuscript has been improved in language.

Specific comments:

Section 1

The introduction could use some restructuring and clarifications. My opinion is that some references are missing, and the addition of these papers will change some of the claims the authors are making in the introduction. Under 'technical corrections' I have provided comments to specific line numbers on this.

The introduction was completely restructured rewritten taking into account the comments provided in 'technical corrections'

Section 2

Lines 128-129: Do the authors have any idea to what degree the station is affected by the anthropogenic emissions? It would be valuable information to add in the text, if it exists? How close is UFS to the skiing

area?

Actually, there exists a study on the influence of anthropogenic activities on the UFS station by Yuan et al. (2019). They detected on weekdays multiple short-term atmospheric CO events and higher atmospheric NO peaks during the daytime (mostly around 09:00 LT), which were interpreted to originate by anthropogenic working activities and less by tourists. During the period the snow samples were collected, the 1 min ambient air eBC data show elevated levels above 1 $\mu\text{g}/\text{m}^3$ only on 20 days and only for short periods of less than 20 min giving a total time of about 160 minutes the station experienced this higher BC pollution levels. This time is less than 1 permille of the total snow sampling period. For those days we have no indications that the snow samples are affected by anthropogenic emissions. However, the results of two samples collected on February 6 and February 17 were discarded from the data, because they show inexplicable high BC mass mixing ratios and absorption coefficients (factor 5 to 10 outside the 95th percentile of the other samples), which indicates a possible contamination from local sources.

Line 136: As the manuscript currently reads, 10 cm of snow was collected after each snowfall. What was the procedure of collecting the snow if there was more (or less) snow in the precipitation event? If it was more than 10 cm, for example, BC particles from the beginning of that snow event would be missing in the analysis. On the opposite, if there was a small snow event, producing only a few centimeters of snow, how was that snowfall sampled? In that event, if 10 cm of snow was sampled, it would include not only the fresh snow (and its particulates), but also more aged particles in the snow, leading to possible differences in the analysis.

We made the procedure clearer by rephrasing the paragraph in Sect. 2.1 as following:

“The snow samples were taken either during or just after snowfall events by scraping off only the top few centimeters of the snowpack to avoid sampling older snow. A metallic hand shovel is used to sample the snow from an area of about 30 x 30 cm into a zipper sealed polyethylene household plastic bag with a volume of 1 L (Toppits, Germany). In this way, snow from the beginning of the snowfall event could be missed, but most of the time the events were accompanied by heavy wind, so that it was impossible to completely sample the fresh snow layer. After collection, the samples were stored at the UFS in a freezer at -18°C until they were transported under frozen conditions to the laboratory at KIT. During six months, 33 samples were taken at the UFS.”

Also, on the topic of the snow sampling, the authors mention that the collection was from a place exposed to wind, and so how did they manage to collect the new precipitation? One would expect the wind to remove this snow (that is typically is not very dense). A table in the supplement of this manuscript could easily be added, providing valuable information about the snow samples, precipitation events, as well as other basic weather parameters during sampling.

In addition to the changes in Sect. 2.1 given above, we replaced Figure 7 with a stacked figure (Figure 8 in the revised manuscript) that highlights the trends in ambient temperature, sunshine duration, snow precipitation and snow height over the period the snow samples were collected at the UFS station. In this Figure also the ambient eBC and the refractory BC concentration of the snow samples is shown to give the reader an overview about the ambient conditions and their changes during the 6 months period of snow sampling.

Line 144: How do the authors know that using the ultrasonic bath to melt the snow sample did not change the structure of the BC particles? (e.g. break the particles apart into smaller sizes, which obviously will have an impact on their optical properties), or the other particles present in the snow also?

We have no information how the ultrasonic bath might affect the microstructure of the particles. However, we followed the recommendations that are given in the literature concerning snow sample analysis to be at least consistent with those studies. We added the following paragraph to the manuscript to make this clearer:

“Aqueous snow/ice sample sonication prior to the analysis is recommended by several groups (e.g. Kaspari et al., 2011; Wendl et al., 2014) although with inconclusive results of the obtained improvements. The melted samples were never refrozen for later analysis as this can result in a significant particle mass loss of up to 60% (Wendl et al., 2014).”

Section 3

Some sentences in the fourth paragraph are already mentioned in the second paragraph (e.g. lines 235- 237 are mentioned in lines 216-219). Technically, I do not see why the information in this fourth paragraph (which ultimately contains more details) could already be incorporated into the second paragraph.

We restructured Section 3 in the revised manuscript to make it more concise.

Lines 225-226: Could you present any quantitative numbers on this minor influence?

The number nebulizing efficiency and the relative humidity are not changing (within a few percent) when varying the cooled section temperature in the low positive temperature range (i.e. 0 to 5°C). However, the efficiency increases and the r.h. decreases for sub-zero temperatures. Operating the nebulizer at a sub-zero cooled section temperature resulted in regular failures of the nebulizer, most likely due to water freezing in the cooled section.

We changed added “a few percent” to the sentence.

Section 4

Lines 263-266: What about adding the size distribution of the fullerene in a figure, to show that the difference in fullerene MAC's could be explained by differences in size?

We added a figure of the size distributions to the manuscript.

Section 5

The results of the snow sample measurements could be highlighted even more. You have 33 samples from one snow season. How do they differ from one another? In Fig. 7 you show how the BC snow concentration varies over this season, what about the air concentration of BC from the station? (it is mentioned that no correlation was found between the snow and air BC concentrations. I would argue that this is shown, possibly in fig. 7 or a different figure). Is there any seasonality in the size distribution of BC particles from snow? I'm not convinced that there is such a clear decrease in the size distribution of the larger BC particles, please elaborate on this to further convince the reader that this is the case. (It is true that since you have taken relatively fresh snow samples, there would be no thawing and freezing cycles, possibly leading to larger BC particles). One example comes to mind where fresh snow BC size distributions were measured (Sinha et al., <https://doi.org/10.1002/2017JD028027>). Although in a different setting, please put your results into context by comparing with this study.

We agree with the reviewer that the presentation and discussion of the snow sample results in the context of concurrent meteorological and ambient aerosol measurements is too short or even lacking in the manuscript. That's why we have replaced Fig. 7 by a stacked plot (Fig. 8 in the revised manuscript) showing maximum and minimum temperature, sunshine duration, precipitation, snow height as well as the air BC mass concentration records over the time period the snow samples were taken.

To discuss the measured rBC snow concentrations in context with these other measurements we added the following paragraph to Section 5:

"This BC concentration is shown in **Error! Reference source not found.c** in conjunction with the eBC mass concentration of ambient air that is routinely measured by the German Federal Environment Agency using a Multi-Angle Absorption Photometer (MAAP). Also, a selection of meteorological data is presented in **Error! Reference source not found.** to highlight the trends in ambient temperature, sunshine duration, snow precipitation and snow height over the period the snow samples were collected at the UFS station. Although there is no clear correlation between the fresh snow samples and ambient air eBC mass concentration, the enhanced air eBC mass concentration observed end of March and beginning of April might have resulted in additional deposition of BC particles in the snow surface that is reflected - with a time lag of several days - in the measured snow refractory BC mass mixing ratio. Interestingly, this period of higher air eBC concentration is distinguished by a low precipitation activity, long sunshine periods as well as frequent daily maximum temperatures above the melting point that resulted in frequent thaw/freeze cycles and, consequently, a gradual decrease of the snow height by 30 to 40 cm. All in all, the enhanced air eBC concentration in conjunction with the meteorological conditions would favor enhanced BC mass concentrations in the fresh snow samples collected after precipitation events within this period or shortly after."

Actually, from the 33 samples we use only 31 samples in the revised manuscript as two samples were discarded due to inexplicable high rBC mass concentrations and absorption coefficients (factor 5 to 10 outside the 95th percentile of the other samples). To investigate a possible seasonality in the measured rBC size distributions of the snow samples, we divided the 31 samples into the three periods (1) November to January with 11 samples, (2) February and March with 11 samples, and (3) April and May with 9 samples. For each period the average rBC size distribution is calculated and is plotted in the updated Fig. 8 (which is Fig. 9 in the revised manuscript).

We thank the reviewer for noticing the Sinha et al. paper. In Fig. 8 of their paper the BC mass size distribution of a fresh snow sample is shown that was collected after a snowfall event at Ny-Ålesund, Svalbard, Norway. We also found the study by Schwarz et al. (2013) very useful as this study presents an averaged rBC mass size distribution of snow samples collected shortly after snowfall events in Colorado, USA (Fig. 1 in their study). Our averaged fresh snow sample size distributions peak at similar mass median diameters (MMD) between 194 and 227 nm compared to the 223 ± 28 nm of the Sinha et al. study and the ~ 220 nm of the Schwarz et al. study. In addition, our BC mass size distributions indicate a non-lognormal shoulder at the upper size limit of our measurement that is in a very good agreement with the Schwarz et al. (2013) samples where the BC mass size distribution was measured up to 2 μm (see Fig. 9 in the revised manuscript which shows a comparison with the Schwarz et al. data). As it is discussed by Schwarz et al. (2013) such a size distribution reflects the typical atmospheric BC distribution at remote locations that is altered by agglomeration and size selection processes during snow formation in the atmosphere.

We also divided the snow samples into the three periods Nov-Jan, Feb-Mar, and Apr-May and present the averaged size distributions of these three periods in Fig. 9 of the revised paper. This clearly shows that here is no significant seasonality in the snow BC data.

We have added the following paragraph to Section 5 to include these comparisons and their

conclusions:

“Figure 9 shows corresponding mass size distributions of the refractory BC concentrations shown in Figure 8c averaged over the periods November to January, February and March, as well as April and May. For comparison purposes, the average size distributions are normalized by the corresponding total mass concentration M_{total} , which was deduced from a lognormal fit. The SP2-derived refractory BC mass size distribution only includes particles up to a mass-equivalent diameter of 560 nm, which means that larger BC particles are not recorded by the SP2. However, the average BC mass size distributions have distinct mode maxima at the mass median diameters (MMD) of 227, 194, and 222 nm for the Nov-Jan, Feb-Mar, and Apr-May periods, respectively. This indicates no strong seasonality in the snow BC mass size distribution even in the Apr-May period where the BC mass concentration in the snow was significantly enhanced (Figure 8c). This further implies that indeed fresh snow was sampled which hasn't experienced thaw/freeze cycles severe enough to induce an agglomeration of the BC particles in the top snow layer. This conclusion is further supported by comparing the average BC mass size distributions of our snow samples with the BC mass size distribution of a fresh snow sample collected after a long-lasting snowfall event at Ny-Ålesund, Svalbard, Norway by Sinha et al. (2018) and with the averaged BC size distribution from five snow samples collected after three snowfall events in the semi-rural and rural surroundings of Denver, CO, USA by Schwarz et al. (2013). Our average fresh snow sample size distributions peak at similar MMD between 194 and 227 nm compared to the 223 ± 28 nm of the Sinha et al. study and the ~ 220 nm of the Schwarz et al. study. In addition, our size distributions indicate a non-lognormal shoulder at the upper size limit of the SP2 measurement that is in a very good agreement with the Schwarz et al. (2013) samples where the refractory BC mass size distributions were measured by a SP2 with modified detector gains up to $2 \mu\text{m}$ (see Figure 9). As pointed out by Schwarz et al. (2013) such snow BC mass size distributions reflect the typical atmospheric BC mass size distribution that is observed at remote locations altered by agglomeration and size selection processes during snow formation in the atmosphere. The good agreement between the mass size distributions of our snow samples and the average distribution of the Schwarz et al. (2013) samples allows us to estimate the refractory BC mass that is contained in the large particle size shoulder outside our measurement range. According to Schwarz et al. (2013) a fraction of 28% of the total BC mass can be attributed to particles with mass-equivalent diameters larger than 600 nm. A mass correction factor of 1.39 is therefore applied to the SP2-derived refractory BC snow concentrations in the following analysis.”

What about the dust concentrations? How did the described Saharan dust episodes influence the BC mass (and the snow samples)?

Although we cannot directly measure the dust concentrations in the snow samples, we can draw some conclusion by analyzing the spectral signature of the snow mass specific absorption cross section of the non-BC particles, i.e. after subtraction the spectral cross section that is expected from the SP2 mass data using the MAC of Fullerene soot (Equation 3 of the revised manuscript). We added a figure (Fig. 12 in the revised manuscript) that shows a comparison of the non-BC spectral absorption cross section with laboratory absorption data for Saharan dust particles. Thus, Saharan dust is a good candidate to explain the observed non-BC light absorption in the snow samples. We did the same comparison with laboratory data of OC, which reveals that OC could also explain the observed non-BC absorption - not only in terms of wavelength dependence but also in terms of variability.

The whole paragraph on the analysis of the spectral absorption analysis has been rewritten to make our argumentation of a significant influence of non-BC particles on the light absorption in snow clearer.

Through the measurement set-up that the authors present, they should have the data necessary to directly derive MAC values for the particles in the snow. How come this was not done? I believe one of the other referees also commented on this. Either the authors provide these MAC values also, and compare (and discuss) that in the manuscript with the data that they already have. If this

is not possible, then it should be stated why, and more emphasized why the approach used currently in the manuscript is utilized. There is evidently other impurities other than the BC particles, which will influence the MAC value for the particles in the snow, but with the other instrumentation available, it should assist in describing those particles (i.e. the OC content).

We did a thorough reanalysis of the snow samples following this strategy:

1. The snow mass specific absorption cross section σ_{abs} [m^2/mL] was deduced from the absorption coefficient b_{abs} [m^{-1}] using the nebulizer flow settings and the nebulizing efficiency (Eq. 1 of the revised manuscript):

$$\sigma_{abs} = 10^{-3} \cdot b_{abs} \cdot R_{neb} / R_{pp} \cdot \varepsilon_{neb}^{-1}$$

2. This snow mass specific absorption cross section is plotted as a function of the refractory BC mass concentrations in a new figure (Fig. 10 of the revised manuscript). Linear regression fits to the data then give the BC mass specific MAC of the snow samples. We found MAC values that are up to a factor of two larger than the MAC of Fullerene soot. A table is added to the manuscript contrasting the mass and optical properties (including the MAC) of Fullerene soot with those of the snow samples.
3. To be comparable with other studies (e.g. Doherty et al., 2010), we calculated the equivalent BC mass concentration c_{BC}^{equiv} , i.e. the amount of BC that would need to be present in the snow to account for the measured absorption, from σ_{abs} using the MAC of Fullerene soot (Equation 2 of the revised manuscript):

$$c_{BC}^{equiv} = \sigma_{abs} / \text{MAC}_{FS}$$

4. We plotted c_{BC}^{equiv} as a function of the refractory BC mass concentration in a new figure (Fig. 11 of the revised manuscript) and found a good correlation of both concentrations but with correlation coefficients of 2.0, 1.9, and 1.4 for 405, 532, and 658 nm, respectively (note that c_{BC}^{equiv} is a function of the wavelength). We conclude from this that there is additional non-BC light absorbing mass in the snow, which is correlated with the BC mass and which has a strong wavelength dependence between the green and the red part of the visible spectrum. This already indicates mineral dust and organic (brown) carbon as possible carriers of this additional absorption.
5. We calculated the snow mass specific absorption cross section of the non-BC particles, σ_{abs}^{nonBC} (Equation 3 in the revised manuscript):

$$\sigma_{abs}^{nonBC} = \sigma_{abs} - c_{BC}^{SP2} \cdot \text{MAC}_{FS} \cdot 10^{-9}$$

We added a figure (Fig. 12 in the revised manuscript) that shows the statistical analysis of the σ_{abs}^{nonBC} for the snow samples and that compares this non-BC spectral behavior with laboratory data for Saharan dust and organic (brown) carbon (see answer to the previous comment).

Line 313: What evidence is there to show that this one sample from March 10th is representative for all of the snow samples? (This sample contains a low amount of BC compared to the other samples and has an enhancement factor of 2.7 compared to the 2.34 presented for the others samples). Either present some evidence that this is representative for all of the samples or emphasize in the manuscript that these additional analyzes (presented in the following paragraphs) were only done to the one sample, and so it is difficult to draw conclusions for all of the snow samples. Ideally, I would argue that additional snow samples would be analyzed from different times during the season in the same way as the one sample from March 10th.

Actually, after the reanalysis of the samples, which includes the correction for missing BC mass in the SP2 measurement, the March 10 sample has a mass concentration $c_{BC}^{SP2}=2.8$ ng/mL and an equivalent BC mass concentration of $c_{BC}^{equiv}=6.0$ ng/ml for $\lambda=532$ nm, which gives an enhancement factor of $\gamma = 2.1$. It is therefore representative for γ , but is on the lower side concerning the c_{BC}^{SP2} and c_{BC}^{equiv} concentrations. We added a mark in the c_{BC}^{equiv} versus c_{BC}^{SP2} plot (Fig. 11 of the revised manuscript) to indicate the representativeness of this sample. As mentioned above, further analyses (especially with the ESEM) are very time consuming and expensive, which we couldn't be invested within the scope of this pilot study. This is now clearly stated in the revised manuscript:

“While these results give a detailed look into the physical and chemical nature of the particles that might contribute the light absorption in the March 10 snow sample, they cannot be used to draw conclusions for all snow samples. Here, further analyses are required that couldn't be conducted within the scope of this pilot study.”

Lines 320-326: Although you discuss it further in the following paragraph, please include some sentence (or sentences) of what these specific results indicate about the snow samples?

Will be added to the revised manuscript.

Line 329: It would be interesting to have some information (even if it is hypothetical) on where this biological information originate from? E.g. Local or long distance?

We changed the terminology in the discussion of the ESEM and WIBS analysis by substituting the term “biological” with “biogenic”. Although we have indications of biological components in the ESEM analysis, like bacteria, pollen and spores, we cannot conclude that all biogenic EDX patterns are due to microorganisms or their fragments. We added a paragraph on possible origins of the biogenic material found in the March 10 sample, mainly in the context of the observed non-BC light absorption by brown carbon.

“However, one question that arises from the above findings is whether the biogenic particles found in the March 10 snow sample can be attributed to BrC, which was shown to be a good candidate for explaining the additional light absorption in the snow samples (**Error! Reference source not found.**). The term “brown carbon” is not clearly defined or characterized and is mainly related to a strong wavelength dependence of the visible light absorption observed in these materials. From a chemical perspective, BrC can generally be divided into humic-like substances (HULIS) and tar balls (Wu et al., 2016). HULIS can be characterised mainly as a mixture of macromolecular organic compounds with various functional groups and are expected e.g. in oxidation processes of biogenic precursors (Wu et al., 2016). Tar balls are emitted from biomass burning and are of spherical, amorphous structure and are typically not aggregated. Moreover, light absorbing organic material and HULIS can be formed from the water-soluble fraction of biomass burning aerosol compounds, and is therefore suggested as an atmospheric process for the formation of light absorbing BrC in cloud droplets (Hoffer et al., 2004). Further examination of snow samples from different locations as well as systematic investigations on the optical behaviour of biogenic particulate matter is therefore necessary to evaluate the influence of biogenic (including biological), BrC and mineral dust on the aerosol absorption properties in the visible spectral range.”

All the comments given in the technical corrections are addressed in the revised manuscript.

Technical corrections:

Lines 29-30: This opening sentence is not structured well. Please revise for a better read.

Line 32: Please remove 'packs' from ice packs. Could say snowpack, but not ice packs here.

Line 32-33: You could argue that a better reference here would be Warren and Wiscombe 1980 [https://doi.org/10.1175/1520-0469\(1980\)037<2734:AMFTSA>2.0.CO;2](https://doi.org/10.1175/1520-0469(1980)037<2734:AMFTSA>2.0.CO;2), look into details of Doherty et al. 2010.

Lines 33-34: How is this sentence different than the previous sentence? I would think that it is better to have this sentence earlier.

Lines 35-36: How does 'this reduction' contribute to the snow-albedo feedback? Please include in the manuscript. What metamorphosis?

Line 41: What 'BC amounts' are you referring to? Please specify.

Lines 44-46: How are permafrost regions also affected? Unclear what you mean how they are affected? Also, after reading the rest of this paragraph, I would argue that you should remove this sentence. Since the rest of the paragraph discusses the Arctic, and these other 'areas' are not brought up again until later in the introduction, it could come then instead.

Line 50: As far as I remember Flanner et al. (2007) did not present any measurements, but based their modeling work on measurements instead.

Line 53: I would argue that you either introduce what the term 'soot' refers to, or stick with only discussing BC.

Line 56: Ice sheet instead of 'ice shield.' Please change also 'extend' to extent.

Lines 55-60: Concerning the Greenland ice sheet, there are also new papers on this topic of impurities, which could be added here (e.g. <https://doi.org/10.5194/tc-10-477-2016>; <https://doi.org/10.5194/tc-11-2491-2017>).

Line 60: Please capitalize a in 'arctic.'

Line 61: Doherty et al. (2010) is already referenced to in the beginning of the sentence.

Line 68: How high amounts of dust? Would be more informative to actually reference to some numbers on this.

Line 69: To my knowledge, Bolch et al. (2012), is incorrectly referenced to here. No studies of BC nor dust were conducted in that paper.

Line 73: Remove 'the' before light absorbing particles.

Lines 77-80: I find this sentence confusing, please rewrite. Mixing the optical method (Doherty et al., 2010), and then the thermos-optical analysis, with the previous sentence about MAC causes some of the confusion. The following paragraph (lines 81-93) dig deeper in each analysis technique and that is appropriate, but the order of this seems strange, in light of the previous paragraph. Actually, I think you could delete the sentences in lines 75-80, and jump right into line 81 and an explanation of the methods (after current sentence ending on line 75).

Lines 92-93: Either remove this sentence or add more information on other instruments and

protocols out there (e.g. DRI and Improve-protocol). I would vote for removing this sentence, I do not think it is very crucial information.

Line 97: I would argue that you do not need quotation marks around Fullerene.

Lines 98-100: This sentence is basically a repeat of the first sentence of this paragraph, please remove.

Lines 102-103: I generally agree with this statement that not much have been reported on the light absorbing properties. But, there has been some publications on this topic addressing it directly and indirectly, e.g. Schwarz et al., 2013 <https://doi.org/10.1038/srep01356>; Zhang et al., 2017 <http://dx.doi.org/10.1016/j.scitotenv.2017.07.100>; Dal Farra et al., 2018 doi: 10.1017/jog.2018.29; Dong et al., <https://doi.org/10.5194/tc-12-3877-2018>. Please add and discuss these references.

Line 104: Please remove 'solar' before albedo.

Lines 103-106: Please clarify the structure by checking the structure. As it currently stands, it is not clear what the main point of the sentence is.

Lines 106-108: Please change this sentence according to the forthcoming changes made for lines 102- 103.

Lines 109-110: The second half of this sentence (starting after 'but') I find problematic. Similar to the comment in lines 102-103, I do believe this topic has been addressed in the literature. For example: Kaspari et al., 2014 (that you already referenced to earlier in the manuscript); Skiles and Painter, 2016 doi: 10.1017/jog.2016.125; Schmale et al., 2017 DOI: 10.1038/srep40501; Zhang et al., 2018 <https://doi.org/10.5194/tc-12-413-2018>, 2018. Please adjust your claim by including these references on this topic.

Line 137: The fact that the snow samples were collected at 'platform 7' does not add any information to a reader unfamiliar with UFS. Please either elaborate on this, or remove.

Line 147: What does 'Enhanced' refer to? Please explain.

Line 150: I do not find the flow rate for this peristaltic pump anywhere. Please add it. Line 184: Please remove the double reference to 'Fischer and Smith (2018).'

Lines 196-198: Do you mean that the solution was prepared in the same way as in Schwarz et al? If so, please correct. Also, I believe the reference should be Schwarz et al. (2012) and not (2010) as it currently reads.

Line 204: How did you 'drop' 30 mL of fullerene solution onto the quartz filters? Please explain more.

Line 260: What did Zhou et al. (2017) refer to with MACreal? Please clarify.

Line 276: Remove 'before' at the end of the sentence.

Line 294: The presented enhancement factors for the different wavelength appear to be averages, please clarify this.

Lines 315-319: The instruments and methodology presented here should be described in section 2. Lines 344-345: This information should be moved to section 2.

Figure 2. I'm not sure how needed this figure is. I actually think that this figure could be integrated into fig. 1.

Figure 8. Why is there is a data gap around 280-300 nm?

Figure 9. This figure is quite busy right now. Could the data points be zoomed in on more? And could the data points be made smaller?

Compare Results

Old File:

acp-2018-1307-manuscript-version2.pdf

19 pages (4.86 MB)

22.01.19, 09:42:28

versus

New File:

acpd-2018-1307_review_06162019.pdf

28 pages (3.78 MB)

16.06.19, 09:38:10

Total Changes

415

Content

169	Replacements
50	Insertions
16	Deletions

Styling and Annotations

180	Styling
0	Annotations

[Go to First Change \(page 1\)](#)

Specifying the light absorbing properties of aerosol particles in fresh snow samples, collected at the Environmental Research Station Schneefernerhaus (UFS), Zugspitze

Martin Schnaiter^{1,4}, Claudia Linke¹, Inas Ibrahim¹, Alexei Kiselev¹, Fritz Waitz¹, Thomas Leisner¹, Stefan Norra², and Till Rehm³

¹Institute of Meteorology and Climate Research, Atmospheric Aerosol Research, KIT, Karlsruhe, Germany

²Institute of Geography and Geoeiology, KIT, Karlsruhe, Germany

³Environmental Research Station Schneefernerhaus (UFS), Zugspitze, Germany

⁴schnaiTEC GmbH, Karlsruhe, Germany

10

Correspondence to: Martin Schnaiter (martin.schnaiter@kit.edu) and Claudia Linke (Claudia.Linke@kit.edu)

Abstract

Light absorbing impurities in snow result in a darkening of the Earth's white snow and ice covers. Airborne particles like mineral dust, volcanic ash or combustion aerosol particles are able to reduce the snow and ice albedo considerably with a very small mass fraction of deposited particles. In this study, a new laboratory method is applied that allows to measure the spectral light absorption coefficient of airborne particles that are released from fresh snow samples by an efficient nebulizing system. Three-wavelength photoacoustic absorption spectroscopy is combined with refractory black carbon (BC) mass analysis to determine the snow mass specific and the BC mass specific absorption cross sections. Fullerene soot in water suspensions are used for the characterization of the method and for the determination of the mass specific absorption cross section of this BC reference material. The analysis of 31 samples collected after fresh snowfall events at a high-altitude alpine station reveal a significant discrepancy between the measured snow mass specific absorption cross section and the cross section that is expected from the BC mass data, indicating that non-BC light absorbing particles are present in the snow. Mineral dust and brown carbon (BrC) are identified as possible candidates for the non-BC particle mass based on the wavelength dependence of the measured absorption. For one sample, this result is confirmed by environmental scanning electron microscopy and by single particle fluorescence measurements, which both indicate a high fraction of biogenic and organic particle mass in the sample.

1. Introduction

Light absorbing atmospheric particles like black carbon (BC), brown carbon (BrC), mineral dust or volcanic ash are eventually removed from the atmosphere by dry and wet deposition. Light absorbing particles that are deposited into snowpack result in a darkening of the otherwise white surface by increased absorption of solar radiation. Because pure snow is the most reflective natural surface on earth, the presence of small amounts of absorptive impurities changes the optical properties of snow resulting in a considerable reduction of the snow albedo (Warren, 1982; Warren and Wiscombe, 1980). In cold fine-grained snow observed BC amounts of ≤ 100 ng/g can reduce the spectral albedo at visible wavelengths by up to 2%, while in melting snow, these reductions can even increase to 6% (Warren and Wiscombe, 1985). Although these numbers seem to be small, they result in a significant impact on the radiation budget via the snow albedo effect (Clarke and Noone, 1985; Flanner et al., 2007), which also

includes secondary effects like rapid snow transformation (e.g. changes in the snow grain size) and the retreat of snow and ice covers in a warming climate. The IPCC reported a global annual mean radiative forcing for anthropogenic BC in snow and ice of $+ 0.04 \text{ W m}^{-2}$ with an uncertainty range of 0.02 to 0.09 W m^{-2} (Boucher et al., 2013). A considerably higher radiative forcing estimate for BC in snow is given in Bond et al. (2013). In their estimate they calculated an effective BC in snow forcing that includes feedback mechanisms, like rapid adjustments of the snowpack as well as the climate response to the snow and ice albedo changes, resulting in a best forcing estimate of $+ 0.13 \text{ W m}^{-2}$ with an uncertainty of 0.04 to 0.33 W m^{-2} .

For a reliable assessment of the radiative forcing by light absorbing impurities in snow and ice, the response of the snow albedo to the presence of light absorbing particles has to be understood from a physical basis. This is not a trivial task as the spectral albedo of snow depends not only on the mass mixing ratio of the absorbing particles in the snowpack, but also on the chemical composition, the microphysical properties, as well as the spectral absorption properties of the particles in addition to the snow grain size distribution and the spatial variations of these parameters (Flanner et al., 2007). While the mass mixing ratio of BC in snow (and also that of mineral dust and organic carbon) has been the subject of many recent studies (e.g. Kaspari et al., 2014; Schmale et al., 2017; Zhang et al., 2018), their microphysical as well as spectral optical properties are still poorly investigated. A few studies exist on the microphysical (Dong et al., 2018; Zhang et al., 2017) as well as optical properties (Dal Farra et al., 2018; Doherty et al., 2010; Kaspari et al., 2014; Schwarz et al., 2013), but these are too sparse from giving a conclusive picture. Further, the optical properties of light absorbing impurities are often indirectly addressed by either applying simplified optical particle models (e.g. Schwarz et al., 2013) or by using mass specific absorption cross sections (MAC) determined for atmospheric particles (e.g. Dong et al., 2018; Zhou et al., 2017). There is a need for more studies that address the question on the microphysical nature and the optical properties of particles in snow and ice. In a large-area study on light absorbing impurities in Arctic snow Doherty et al. (2010) applied the integrating-sandwich with integrating sphere technique (ISSW; Grenfell et al., 2011) to measure the snow mass specific spectral absorption cross section, σ_{abs} , on filter samples. The ISSW is an improved version of the original integrating plate (IP) filter method that was used in the pioneering work of Clarke and Noone (1985) to determine the BC in the Arctic snowpack. Although their method measures σ_{abs} , they used a fixed MAC for BC and assumed fixed absorption Angström exponents for BC and non-BC to calculate the BC mass mixing ratios and the fraction of non-BC particles in the snow, respectively. However, large biases have been revealed in laboratory tests of the ISSW when non-BC absorbing and purely light scattering particles are co-deposited on the filter (Schwarz et al., 2012). This indicates a significant cross-sensitivity of the ISSW-determined σ_{abs} to particle light scattering.

In the present study we used a different approach to measure σ_{abs} by applying three-wavelength photoacoustic spectroscopy on re-aerosolized snow samples. Photoacoustic aerosol spectroscopy is not prone to light scattering artefacts and, therefore, gives reliable results also in the presence of light scattering impurities. As a pilot study for this approach, freshly fallen snow was collected at the alpine research station Schneefernerhaus over a period of six months in Winter 2016/2017. Particulate impurities in the samples were re-aerosolized in the laboratory and were concurrently measured by a single particle soot photometer (SP2) as well as by a homebuilt three-wavelength photoacoustic spectrometer (PAAS- 3λ) to determine σ_{abs} and the BC mass specific MAC of the snow impurities. Suspensions of Fullerene soot in water were prepared as a standard for melted snow and were used to characterize the nebulizer efficiency and to determine the PAAS- 3λ detection sensitivity. From these measurements, also the MAC of the Fullerene soot standard was deduced and was compared with the MAC of the snow samples.

Sample preparation, test particle properties and experimental setup are given in Sect. 2. Sect. 3 describes the characterization of the nebulizer at different operational settings and gives the efficiency of the nebulizer in terms of particle number and mass concentrations. The MAC of the Fullerene soot standard is presented in Sect. 4. Measurement results of the snow samples are discussed Sect. 5 followed by conclusions given in Sect. 6.

2. Experimental

2.1 Snow samples

The snow samples used in this study originate from the Environmental Research Station Schneefernerhaus (UFS). The station is located at a latitude of $47^{\circ} 25' 00''$ N, a longitude of $10^{\circ} 58' 46''$ E and an altitude of 2650 m a.s.l. During winter the UFS is situated in the free troposphere most of the time with low boundary layer influence (Gilge et al., 2010) but can be occasionally affected by long range transported Saharan dust plumes (Flentje et al., 2015) or in rare events by transatlantic aerosol transport (Birmili et al., 2010). However, the station is located within a skiing and hiking resort and is therefore sporadically affected by local anthropogenic emissions during daytime, e.g. from snow groomers during the skiing season. Yuan et al. (2019) report multiple short-term atmospheric CO events and higher atmospheric NO peaks during the weekdays (mostly around 09:00 LT) at the station. Disregarding these local pollution events at the station, the multi-annual median BC mass concentration is $0.1 \mu\text{g}/\text{m}^3$ and is typically well below this value during the winter months (Sun et al., 2019).

Snow samples were collected during a time period from December 2016 to May 2017. During this time period basic meteorological data of precipitation, maximum and minimum temperatures, sunshine duration and wind speed are provided by the German Meteorological Service (DWD). Aerosol parameters like number concentrations from condensation particle counter (CPC) and optical particle counter (OPC) instruments, equivalent BC mass concentrations from multi-angle absorption photometer (MAAP) measurements as well as dust loads are provided by the German Federal Environment Agency (UBA) and the German Meteorological Service (DWD). The snow samples were taken either during or just after snowfall events by scraping off only the top few centimeters of the snowpack to avoid sampling older snow. A metallic hand shovel is used to sample the snow from an area of about $30 \times 30 \text{ cm}$ into a zipper sealed polyethylene household plastic bag with a volume of 1 L (Toppits, Germany). In this way, snow from the beginning of the snowfall event could be missed, but most of the time the events were accompanied by heavy wind, so that it was impossible to completely sample the fresh snow layer. After collection, the samples were stored at the UFS in a freezer at -18°C until they were transported under frozen conditions to the laboratory at KIT. During six months, 33 samples were taken at the UFS.

Right before the analysis, which is described in the following sections, approximately 30 mL snow is detached from the plastic bag and is put in a glass beaker for further treatment. This subsample is then melted by sonication in an ultrasonic bath (EMAG Technologies, Germany) at room temperature for about 5 minutes. Sonication during the melting process should help to avoid particle adhesion to the wall of the glass beaker. Aqueous snow/ice sample sonication prior to the analysis is recommended by several groups (e.g. Kaspari et al., 2011; Wendl et al., 2014) although with inconclusive results of the obtained improvements. The melted samples were never refrozen for later analysis as this can result in a significant particle mass loss of up to 60% (Wendl et al., 2014).

2.2 Setup of instruments

The experimental setup consisting of a Marin-5 Enhanced Nebulizer System (Teledyne CETAC Technologies, USA), a self-built three-wavelength photoacoustic aerosol absorption spectrometer (PAAS-3λ, Linke et al., 2016) and a single particle soot photometer (SP2, Droplet Measurement Technologies, USA) is shown in Figure 1. The liquid samples are fed by a peristaltic pump (ISM795, ISMATEC, Wertheim, Germany) equipped with Tygon tubing (ID 0.76 mm, E-LFL, Fisher Scientific, USA) into a concentric pneumatic glass nebulizer (“MicroMist 500” with a critical orifice of 500 μm), which is positioned inside of the Marin-5 nebulizer. The glass nebulizer consists of a capillary that directs the liquid sample to the nebulizer tip where a concentric sheath flow of pressurized synthetic air disperses the supplied liquid sample into a spray (Katich et al. 2017). The optimum specified liquid sample flow rate of the glass nebulizer, which is set on the peristaltic pump, is $R_{pp}=0.5$ mL/min.

120 The generated spray is released into the nebulizing chamber of the Marin-5 nebulizer with the maximum specified gas flow rate of $R_{neb}=1.1$ L/min (see Figure 2). The spray enters the heated section of the chamber where the water is evaporated forming a moist aerosol of residual particles. This aerosol comprises refractory aerosol particles and residues from soluble material that were contained in the liquid sample. Subsequently, the aerosol passes the cooled section of the chamber where excess water is eliminated from the sample flow by condensation to the chamber

125 walls, so that the bulk of water vapour in the moist aerosol is drained before the particles leave the nebulizer. The aerosol that exits the nebulizer is then directed through a homebuilt silica gel dryer to reduce the relative humidity of the aerosol flow below 20% r.h. Finally, sample flows for the SP2 and the PAAS-3λ are taken from the aerosol flow, which is otherwise exhausted to the ambient.

130 The SP2 was used to determine the refractory black carbon (BC) mass concentration c_{BC}^{SP2} of the BC suspension standards and the snow samples. The instrument is typically operated with a sample flow rate of 0.12 L/min. For single particle mass determination, the two incandescence channels of the instrument are calibrated with Fullerene soot particles (Alfa Aesar, #40971, lot #F12S011) size selected by a differential mobility analyser (DMA) in the range of 100 nm to 450 nm, corresponding to single particle refractory BC masses of about 0.5 fg to 30 fg. Note that this “Fullerene soot” material actually contains only a minor mass fraction of Fullerenes of less than 10%

135 140 (Laborde et al., 2012a). The gains of the two incandescence channels of the SP2 are adjusted in a way that they cover a combined volume-equivalent size range from 60 to 560 nm (Laborde et al., 2012b). For quantifying the number efficiency of the nebulizer, number concentrations of non-absorbing PSL particles are determined from the SP2 single particle scattering data. For analysis of the SP2 data, the software toolkit developed and provided by Martin Gysel from the Paul Scherrer Institute, Switzerland is used (Gysel et al., 2011).

145 150 The PAAS-3λ is a single cavity three-wavelength photoacoustic aerosol absorption spectrometer, which has been designed and built at KIT and which is currently marketed by schnaiTEC GmbH. The instrument concept and working principle are described in detail in Linke et al. (2016). Briefly, to measure the absorption coefficient b_{abs} of aerosols, a controlled sample flow of 0.85 L/min is led through the acoustic resonator of the instrument. This open-ended cylindrical cavity has a diameter of 6.5 mm and a length of 49 mm resulting in a fundamental acoustic resonance frequency of about 3200 Hz. Acoustic buffers of 24.5 mm length and 78 mm diameter are attached to both ends of the cavity to filter acoustic disturbances that may exist in the frequency range of the resonator.

155 Possible disturbances comprise noise generated in the flow system as well as ambient sound. The photoacoustic cell composed of the acoustic resonator and the buffers has a total volume of 236 cm³. The PAAS-3λ system was developed to determine the absorption coefficients at three wavelengths across the visible spectral range. Three lasers (Dragonlaser, Changchun, China), modulated at the resonance frequency of the acoustic cavity, are used in

this study. The lasers have emitting wavelengths of 405, 532, and 658 nm and generate modulated emission power of 100, 150 and 130 mW, respectively. The modulation frequency has a duty cycle of 50% and is tuned to the resonance frequency of the acoustic cavity on a daily basis. The detection limit (2σ) of this setup was derived from an Allan deviation analysis of long-term background signal measurements similar to the analysis presented in Fischer and Smith (2018). The Allan deviation plot for the three PAAS-3 λ wavelengths is shown in Figure 3. According to this analysis, the PAAS-3 λ instrument has a 2σ detection limit in the range of 1.2 to 2.1 1/Mm for all three wavelengths and for a typical averaging time of 60 seconds.

2.3 PSL particles

The characterisation of the particle number efficiency of the nebulizer and the daily performance control was performed with monodisperse polystyrene latex (PSL) particles (Postnova Analytics GmbH, Landsberg am Lech, Germany) with nominal diameters of 240 ± 5 nm and 304 ± 5 nm. The particle number concentration within these suspensions is about $3 \cdot 10^8$ 1/mL. A diluted PSL standard suspension sample was prepared daily by pipetting 1 mL suspension into a 100 mL graduated flask filled with Nanopure water.

2.4 Fullerene Soot Standards

Suspensions of known Fullerene soot mass concentrations were prepared to determine the particle mass efficiency ε_{neb} of the nebulizer. The material has been widely used to calibrate SP2 instruments (including the present study) as it gives a sensitivity that is similar to Diesel soot (Laborde et al., 2012a). A stock suspension of Fullerene soot particles (Alfa Aesar, USA; stock #40971, lot #F12S011) suspended in Nanopure water was stored in a 250 mL graduated glass bottle with polypropylene cap (Simax, Czech Republic) for several days to allow larger particles to settle out of the suspension. From this stock suspension the supernatant suspension was taken to (a) determine the Fullerene soot mass concentration gravimetrically and to (b) prepare diluted Fullerene soot standard suspensions for daily particle mass efficiency control of the nebulizer.

For the gravimetric analysis of the settled stock suspension two empty quartz fibre filters (MK360, Ahlstrom Munksjö, Finland) were dried over night at 50°C, stored in a dehydrator for 2 hours and weighed with a microbalance (M3P, Sartorius, Germany). Then 30 mL of the supernatant suspension were extracted from the stock Fullerene soot suspension and were dropped on both quartz filters. The filters were then temperature treated the same way as the empty filters before being weighed again. From the gravimetric Fullerene soot mass, the mass concentration of the stock suspension was determined to be 5.8 ± 2.6 $\mu\text{g/mL}$ (mean $\pm 1\sigma$; N=2). Four Fullerene soot standard suspensions for the determination of the mass efficiency ε_{neb} of the nebulizer were prepared on each measurement day from the stock suspension. This was performed in two dilution steps resulting in samples of Fullerene soot suspended in Nanopure water with nominal mass concentrations of $c_{FS} = 11.5 \pm 2.5$, 23 ± 7.3 , 34.5 ± 6.3 and 46 ± 7.7 ng/mL. Note that the given uncertainty range is based on the analysis of the SP2 mass measurements acquired during the characterization of the Marin-5 nebulizing efficiency (Sec. 3) and does not reflect possible systematic biases in the above gravimetric analysis of the stock suspension and the subsequent dilution process.

3. Characterization of the nebulizer

Particles suspended in liquid samples are not completely dispersed during the nebulizing process in the Marin-5 nebulizer but are partially lost in the drain water of the instrument. In order to characterize the Marin-5 dispersion efficiency the nebulizer settings were varied while measuring the particle output by a CPC. In this characterization 195 the operation recommendations given by Katich et al. (2017) for applying the Marin-5 in snow sample analyses were mainly adopted. However, a minimum gas flow rate of $R_{neb}=0.97$ L/min is necessary in the present study to simultaneously operate the SP2 and the PAAS-3 λ downstream the Marin-5. Also, the relative humidity of the Marin-5 output flow is an important property here as reliable photoacoustic measurements of aerosol systems require a relative humidity below $\sim 30\%$ (Langridge et al., 2013). The particle output (in terms of particle number 200 and particle mass) and the relative humidity depend on the R_{pp} and R_{neb} flow rates and the temperatures of the heated and cooled sections of the nebulizing chamber. As a starting point of the Marin-5 characterization the nebulizer parameters were set to heating and cooling temperatures of 120°C and 5°C, respectively, the maximum specified input air flow rate of $R_{neb}=1.1$ L/min, and a liquid sample flow rate of $R_{pp}=0.08$ mL/min. Each parameter, except R_{neb} , was varied while keeping the others constant. It turned out that the temperature of the 205 cooled section of the chamber has only a minor influence of a few percent on the dispersion efficiency and the relative humidity in the output flow.

In Figure 4, the PSL particle number nebulizing efficiency and the relative humidity of the Marin-5 exit flow are shown as a function of the liquid sample flow rate R_{pp} of the nebulizer. From Figure 4 it is clear that the higher the applied sample flow rate R_{pp} the higher the relative humidity at the exit at a fairly constant efficiency of around 210 36%. Note that the observed constant nebulizing efficiency reflects a nearly linear correlation between the PSL number concentration at the nebulizer exit and the liquid supply rate R_{pp} at the input. Even for the lowest R_{pp} of 0.08 mL/min the relative humidity approaches 50% and is therefore far above the threshold humidity of 30% for unbiased photoacoustic measurements. Therefore, the silica gel aerosol dryer downstream the Marin-5 is a prerequisite in the Fullerene soot and snow sample analysis with the PAAS-3 λ instrument. The PSL number 215 concentration and relative humidity behave in a similar way when R_{pp} is kept constant at 0.16 mL/min and the temperature of the heated section of the chamber is varied between 110 and 150°C, i.e. higher values with higher temperatures (not shown here). As a result of this characterization the liquid sample flow rate was set to $R_{pp}=0.32$ mL/min in the Fullerene soot and snow sample analyses in order to generate a sufficient absorption signal in the PAAS-3 λ while the aerosol can still be dried to a relative humidity below 30%. The nebulizer temperatures were 220 set to 120°C and 5°C for the heated and cooled section, respectively.

With the above settings and the setup shown in Figure 1, the mass nebulizing efficiency $\varepsilon_{neb} = c_{BC}^{SP2} / c_{FS} \cdot R_{neb} / R_{pp}$ of the Marin-5 nebulizer was derived from measurements using the Fullerene soot standard suspensions described in Sec. 2.4. In Figure 5 the detected SP2 mass concentrations c_{BC}^{SP2} are shown for the four Fullerene soot standards which were daily prepared. The mass nebulizing efficiency was determined to be 39% from these 225 measurements, which is in a very good agreement with the findings of Katich et al. (2017) for similar settings.

Figure 6 shows the average mass size distributions of the four Fullerene soot suspension standards used in the characterization of the Marin-5 mass nebulizing efficiency ε_{neb} shown in Figure 5. Each size distribution is an average over 8 individual suspensions that were prepared on a daily basis. The measured mass size distribution of

each of the 32 individual suspensions was fitted by a lognormal function to get the mass-equivalent median diameter (MMD), the width of the distribution (i.e. geometric standard deviation σ_g), as well as the integrated mass concentration, c_{BC}^{SP2} . Note that the integrated mass concentration c_{BC}^{SP2} from the lognormal fit was used in determination of ε_{neb} and the Fullerene soot mass absorption cross sections, MAC_{FS} , in Sec. 4. This is necessary as the summed particle mass from the SP2 measurement alone ignores particles with sizes larger than 560 nm, which represent a mass fraction of about 10% (see Figure 6). The suspensions show a very stable MMD of 227 ± 230 3.7, 226 ± 1.7 , 228.5 ± 2.5 , and 229 ± 1.7 nm and σ_g of 1.57 ± 0.018 , 1.56 ± 0.024 , 1.57 ± 0.017 , and 1.57 ± 0.016 235 for the 11.5, 23, 34.5, and 46 ng/mL suspensions, respectively with a MMD of 228 ± 3 nm and a σ_g of 1.57 ± 0.018 when averaging over all 32 samples (Table 1).

4. Specific mass absorption cross sections (MAC_{FS}) of Fullerene soot

Simultaneously to the BC mass concentration measurements with the SP2, the absorption coefficients b_{abs} of the 240 Fullerene soot suspensions were measured for the three PAAS-3λ wavelengths. Both measurements together enable the determination of the mass specific absorption cross section $MAC_{FS} = b_{abs}/c_{BC}^{SP2}$ of airborne Fullerene soot at 405, 532, and 658 nm. In Figure 7, the absorption coefficients b_{abs} are plotted against the SP2-derived BC 245 mass concentrations c_{BC}^{SP2} of the Fullerene soot suspension standards. Linear regression fits of the data result in MAC_{FS} values of 10.5 ± 3.2 m²/g, 9.5 ± 2.2 m²/g, and 8.6 ± 3.3 m²/g for 405, 532, and 658 nm, respectively. The MAC_{FS} at 532 nm is comparable to the value of 8.84 m²/g given by Schwarz et al. (2012) for Fullerene soot (lot #F12S011) deduced from ISSW measurements, but is significantly higher than the 6.1 ± 0.4 m²/g (mean $\pm 2\sigma$) measured recently by photoacoustic absorption spectroscopy for size selected Fullerene soot particles by Zangmeister et al. (2018). They used a combination of a differential mobility analyzer (DMA) and an aerosol 250 particle mass analyzer (APM) to select Fullerene soot particles within a narrow mass range from aerosol generated by an atomizer. Their MAC_{FS} of 6.1 m²/g, which is given for a wavelength of 550 nm, a mobility-equivalent diameter of 350 nm, and for a particle mass of $16.6 \cdot 10^{-15}$ g, corresponds to a volume-equivalent diameter of 264 nm using a density of 1.72 g/cm³ of Fullerene soot (Kondo et al., 2011). Although, this diameter is not very different to the MMD of 228 nm of the Fullerene soot suspensions used here, part of the observed discrepancy can be attributed to the different sizes as the MAC is strongly depending on the particle diameter for particles larger 255 than about 200 nm (e.g. Moosmüller et al., 2009). To be comparable, we measured the MAC_{FS} of size selected Fullerene soot particles in a separate study by adding a DMA behind the Marin-5 in the setup shown in Figure 1. A MAC_{FS} of 8.6 m²/g was measured for the mobility-equivalent diameter of 350 nm, which is still ~40% larger 260 than the MAC_{FS} given by Zangmeister et al. (2018) for the same diameter. However, they used an APM to measure the BC mass, while a SP2 was used here to deduce the refractory BC mass. According to Laborde et al. (2012a), the Fullerene soot product shows a variability from batch to batch, which results in a SP2 calibration uncertainty of up to 15% (actually only two batches were compared; lot #F12S011 and lot #L18U002). They explained the 265 differences in the SP2 response (i.e. the calibration curves) by a substantial non-refractory coating in case of the L18U002 batch that could be identified by thermodenudging the samples. Assuming that lot #W08A039 used in Zangmeister et al. (2018) has a similar coating, this would increase the APM mass measurement by about 15% compared to the SP2-derived BC mass of lot # F12S011 used in the present study. This in turn would increase the MAC_{FS} from 6.1 m²/g reported by Zangmeister et al. (2018) to about 7 m²/g when using only the refractory BC

mass fraction in the calculation of the MAC_{FS} . This assumption reduces the discrepancy between the two MAC_{FS} values to 35%, which is within the uncertainty range of $\pm 2.2 \text{ m}^2/\text{g}$ for our 532 nm value. It is further conceivable that different batches of the Fullerene soot material have different electronic band structure (i.e. refractive index) and/or fractal aggregate structures that both change the absorption cross section of the particles at a constant particle mass (e.g. Liu et al., 2019; Zangmeister et al., 2018). Figure 17 shows an electron micrograph of a typical Fullerene soot aggregate sampled from the dry aerosol output of the Marin-5 nebulizer. Thus, the Fullerene soot particles do not have a simple fractal aggregate structure, but are rather complex-structured with polydisperse monomer sizes, monomer nonsphericity (irregularity), necking, and overlapping, which all have a significant impact on the optical particle properties (including the absorption cross section) compared to the idealized fractal aggregate (Teng et al., 2019). Since these microphysical details of the soot particles are very sensitive to the actual formation and subsequent treatment conditions (Gorelik et al., 2002), it is conclusive that the MAC_{FS} has an even higher variability between different Fullerene soot batches compared to what is expected from the SP2 mass sensitivity only.

The wavelength dependence of the aerosol light absorption, expressed by the so-called absorption Angström exponent (AAE), was determined to be 0.46 ± 0.07 for the used Fullerene soot suspensions by analysing the b_{abs} data for the 405 and 658 nm wavelengths. This AAE is close to the ~ 0.6 reported by Baumgardner et al. (2012) for Fullerene soot derived from multiwavelength PSAP and Aethalometer measurements and it is within the range of the 0.54 ± 0.06 determined by Zhou et al. (2017) from ISSW spectrometer measurements on Fullerene soot filter samples in the 450 nm to 750 nm spectral range. However, it is significantly lower than the 0.92 ± 0.05 given by Zangmeister et al. (2018) for Fullerene soot lot #W08A039. Here again, we have to take into account that Zangmeister et al. (2018) analyzed size segregated absorption spectra and their AAE is given for a mobility-equivalent diameter of 350 nm. Analyzing our size segregated measurements gives an AAE of 0.82 ± 0.02 for the same mobility-equivalent diameter, which is close but smaller than the Zangmeister et al. value, further supporting the above assumption that there is a difference in the chemical as well as physical (including optical) properties between different batches of the Fullerene soot product.

In conjunction with the b_{abs} detection limit of 2.1 l/Mm given in Sec. 2.2 for the PAAS-3λ and the mass nebulizing efficiency ε_{neb} of the Marin-5 nebulizer given in Sec. 3, the MAC_{FS} analysis shown in Figure 7 can be used to assess the detection limit of the PAAS-3λ in terms of the BC mass mixing ratio in the snow. A conservative estimate that also accounts for the uncertainties in the preparation and quantification of the Fullerene soot suspension standards gives a lower BC mass mixing ratio of 4 ng/mL that can be optically detected by the PAAS-3λ within the setup shown in Figure 1. Therefore, the method presented here should be suitable to analyse the visible light absorption of BC snow impurities for continental as well as for the most of the Arctic areas (e.g. Table 1 in Warren (2019)).

300 5. Results and discussion of the snow sample measurements

The instrumental setup was used to measure a set of 33 snow samples from the UFS in the same way as the Fullerene soot standards before. The results of two samples were discarded from data presented here, because they show inexplicable high BC mass concentrations and absorption coefficients (factor 5 to 10 outside the 95th percentile of the other samples), which indicates a possible contamination from local sources. The measured

305 refractory BC mass concentrations of the aerosolized snow samples were corrected for the Marin-5 nebulizing efficiency to determine the BC mass concentrations per mL volume of melted snow. This BC concentration is shown in Figure 8c in conjunction with the eBC mass concentration of ambient air that is routinely measured by the German Federal Environment Agency using a Multi-Angle Absorption Photometer (MAAP). Also, a selection of meteorological data is presented in Figure 8 to highlight the trends in ambient temperature, sunshine duration, 310 snow precipitation and snow height over the period the snow samples were collected at the UFS station. Although there is no clear correlation between the fresh snow samples and ambient air eBC mass concentration, the enhanced air eBC mass concentration observed end of March and beginning of April might have resulted in additional deposition of BC particles in the snow surface that is reflected - with a time lag of several days - in the measured snow refractory BC mass mixing ratio. Interestingly, this period of higher air eBC concentration is distinguished 315 by a low precipitation activity, long sunshine periods as well as frequent daily maximum temperatures above the melting point that resulted in frequent thaw/freeze cycles and, consequently, a gradual decrease of the snow height by 30 to 40 cm. All in all, the enhanced air eBC concentration in conjunction with the meteorological conditions would favor enhanced BC mass concentrations in the fresh snow samples collected after precipitation events within this period or shortly after. Figure 9 shows corresponding mass size distributions of the refractory BC 320 concentrations shown in Figure 8c averaged over the periods November to January, February and March, as well as April and May. For comparison purposes, the average size distributions are normalized by the corresponding total mass concentration M_{total} , which was deduced from a lognormal fit. The SP2-derived refractory BC mass size distribution only includes particles up to a mass-equivalent diameter of 560 nm, which means that larger BC particles are not recorded by the SP2. However, the average BC mass size distributions have distinct mode maxima 325 at the mass median diameters (MMD) of 227, 194, and 222 nm for the Nov-Jan, Feb-Mar, and Apr-May periods, respectively. This indicates no strong seasonality in the snow BC mass size distribution even in the Apr-May period where the BC mass concentration in the snow was significantly enhanced (Figure 8c). This further implies that indeed fresh snow was sampled which hasn't experienced thaw/freeze cycles severe enough to induce an agglomeration of the BC particles in the top snow layer. This conclusion is further supported by comparing the 330 average BC mass size distributions of our snow samples with the BC mass size distribution of a fresh snow sample collected after a long-lasting snowfall event at Ny-Ålesund, Svalbard, Norway by Sinha et al. (2018) and with the averaged BC size distribution from five snow samples collected after three snowfall events in the semi-rural and rural surroundings of Denver, CO, USA by Schwarz et al. (2013). Our average fresh snow sample size distributions peak at similar MMD between 194 and 227 nm compared to the 223 ± 28 nm of the Sinha et al. study and the ~ 220 335 nm of the Schwarz et al. study. In addition, our size distributions indicate a non-lognormal shoulder at the upper size limit of the SP2 measurement that is in a very good agreement with the Schwarz et al. (2013) samples where the refractory BC mass size distributions were measured by a SP2 with modified detector gains up to $2 \mu\text{m}$ (see Figure 9). As pointed out by Schwarz et al. (2013) such snow BC mass size distributions reflect the typical atmospheric BC mass size distribution that is observed at remote locations altered by agglomeration and size 340 selection processes during snow formation in the atmosphere. The good agreement between the mass size distributions of our snow samples and the average distribution of the Schwarz et al. (2013) samples allows us to estimate the refractory BC mass that is contained in the large particle size shoulder outside our measurement range. According to Schwarz et al. (2013) a fraction of 28% of the total BC mass can be attributed to particles with mass-equivalent diameters larger than 600 nm. A mass correction factor of 1.39 is therefore applied to the SP2-derived 345 refractory BC snow concentrations in the following analysis.

For the assessment of the albedo effect of particulate impurities in snow surfaces the spectral absorption that is contained in the snow has to be quantified. As already mentioned in the introduction this is usually achieved by quantifying the mass mixing ratio of light absorbing particles in the snow and applying a mass specific absorption cross section to that particle mass resulting in a total absorption cross section per snow mass σ_{abs} (given in m^2/mL).

350 With the measurement setup given in Figure 1, this quantity is directly assessable. To deduce σ_{abs} the measured absorption coefficient b_{abs} [m^{-1}] of the aerosol released from the snow sample is converted by following equation

$$\sigma_{abs} = 10^{-3} \cdot b_{abs} \cdot R_{neb}/R_{pp} \cdot \varepsilon_{neb}^{-1}, \quad (1)$$

with R_{neb} and R_{pp} the air and liquid sample flow rates of the nebulizer, and ε_{neb} the nebulizing efficiency. A unit conversion factor of 10^{-3} is necessary because b_{abs} is given as [m^2/m^3], while R_{neb} is given as [L/min]. σ_{abs}

355 values are calculated for the 31 UFS snow samples using Eq. (1) and are plotted in Figure 10 as a function of the corresponding refractory BC mass concentrations c_{BC}^{SP2} , which were corrected for the missing larger particle mass in accordance with the discussion above. This results in a good correlation between the snow mass specific absorption cross section σ_{abs} and the refractory BC mass concentration of the snow samples with the mass absorption cross section, MAC, of the snow particles as correlation factor. In Table 1, the MAC values of the snow

360 samples are compared with those determined for the Fullerene soot suspension standards. It is clear from Table 1 that the MAC of the snow particles is significantly larger than the MAC of the Fullerene soot with wavelength-dependent “enhancement” factors of 2.0, 1.9, and 1.4 for 405, 532, and 658 nm, respectively. This observation suggests that (i) the BC particles in the snow are thickly coated with transparent or low absorbing material that results in a real absorption amplification of the internally mixed particles by the so called lensing effect (e.g.

365 Schnaiter et al., 2005), and/or (ii) part of the absorbing aerosol mass in these samples might be mineral dust or brown carbon that is co-deposited with the BC mass and that has a significant and strong wavelength-dependent mass absorption cross section in the visible spectral region (Schnaiter et al., 2006; Wagner et al., 2012). Both explanations are conclusive for atmospheric aerosol observed at a remote location like the UFS. Although the wavelength-dependence of the observed absorption “enhancement” suggests an insignificant impact from thickly 370 coated BC particles – as this should show a larger absorption amplification in the red compared to the blue spectral range (Schnaiter et al., 2005) – the lensing effect is strongly depending on the actual coating thickness, the coating material, the composite particle size, and the geometrical particle configuration (Kahnert et al., 2012; You et al., 2016). Further, the mean AAE of the snow samples for the spectral ranges from 405 to 658 nm and 532 to 658 nm is 1.20 ± 0.85 and 2.10 ± 2.24 , respectively, which is significantly larger but more varying than 0.46 ± 0.07 and 375 0.60 ± 0.12 deduced for the Fullerene soot suspensions for the same spectral ranges (Table 1). This suggests that it is more likely that the BC particles in the snow are accompanied by non-BC aerosol particles in varying amounts that induce additional absorption predominantly in the blue and green part of the visible spectrum.

Doherty et al. (2010) analyzed spectroscopic measurements of Arctic snow samples using the ISSW photometer to deduce the equivalent BC mass concentration c_{BC}^{equiv} , i.e. the amount of BC that would need to be present in the 380 snow to account for the measured absorption. With the concurrent PAAS-3λ and SP2 measurements presented here, this quantity can be deduced in a similar way for the fresh snow samples from the UFS. For this purpose, the Fullerene soot absorption-equivalent mass concentration c_{BC}^{equiv} was determined from the snow mass specific absorption cross section σ_{abs} (Eq. 1) by applying the MAC_{FS} determined for the Fullerene soot suspensions (Sect. 4 and Figure 7)

$$c_{BC}^{equiv} = \sigma_{abs}/MAC_{FS} . \quad (2)$$

In Figure 11, the deduced c_{BC}^{equiv} values for the 31 snow samples are plotted as a function of the c_{BC}^{SP2} mass concentrations. Interestingly, the two quantities are well correlated (R^2 between 0.89 and 0.93) with correlation coefficients $\gamma = \Delta c_{BC}^{equiv} / \Delta c_{BC}^{SP2}$ of 2.0, 1.9, and 1.4 for the 405, 532, and 658 nm wavelength, respectively, i.e. substantially different from unity. This indicates that (i) there is a significant fraction of light absorption in the particle mass that cannot be attributed to refractory BC, (ii) the reason for this additional absorption is correlated with the BC mass, and (iii) the additional absorption has a strong wavelength dependence between the blue and red part of the visible spectrum. To further elaborate this observation the snow mass specific absorption cross section of the non-BC particles, σ_{abs}^{nonBC} , was calculated from σ_{abs} of all particles

$$\sigma_{abs}^{nonBC} = \sigma_{abs} - c_{BC}^{SP2} \cdot MAC_{FS} \cdot 10^{-9} , \quad (3)$$

395 with MAC_{FS} the mass absorption cross section of Fullerene soot and a conversion factor of 10^9 [ng/g]. Figure 12 shows the statistical analysis of σ_{abs}^{nonBC} for the 31 snow samples of the present study. Thus, the non-BC particles show an absorption characteristic with a gradual increase of σ_{abs}^{nonBC} with decreasing wavelength, which is accompanied by a strong increase of its variability. Again, this points to co-deposited aerosol mass that predominantly absorbs in the blue and green part of the visible spectrum. As already mentioned, possible 400 candidates for this additional light absorption are mineral dust and BrC.

Saharan dust events are routinely monitored by DWD based on a combination of particle size distribution and calcium (Ca^{2+}) concentration measurements, which defines the Saharan Dust Index (SDI; Flentje et al., 2015). Based on the latest SDI inventory¹, the UFS station was influenced by Saharan dust on approximately 20 days within the period January to May 2017. Therefore, it is conclusive that Saharan dust likely influences the light 405 absorption of the UFS snow samples. In an aerosol chamber study Wagner et al. (2012) deduced the complex refractive index, $m = n + ik$, of Saharan soil dust samples collected in a source region in southern Morocco during the SAMUM-1 field project (Heintzenberg, 2009). In Figure 12, σ_{abs}^{nonBC} is compared with the average spectrum of the imaginary part, k , of the refractive index deduced for the three Moroccan dust samples of the Wagner et al. (2012) study. Such a comparison is reasonable as the absorption cross section of mineral dust is dominated by the 410 imaginary part of the refractive index (as well as the particle size distribution) and less by the real part. While the Saharan dust spectrum closely resembles the spectral signature of σ_{abs}^{nonBC} with a very good match of the average values, the low spectral resolution and the high statistical variation of the σ_{abs}^{nonBC} data might also allow for a different interpretation. Schnaiter et al. (2006) used a propane diffusion flame to generate carbonaceous aerosol particles with different organic carbon (OC) mass fractions in the range from about 10 to 70%. They found a strong 415 correlation between the OC mass fraction and the wavelength dependence of the aerosol absorption with AAE between 1 and as large as 9. Consequently, the particulate combustion emissions had different colors from black to brown to yellow, therefore representing brown carbon aerosol. Two examples from the Schnaiter et al. (2006) study are shown in Figure 12 to highlight a possible contribution of BrC to the non-BC absorbing aerosol mass in the snow samples. These two examples with OC mass fractions of 30 and 50% and mass specific absorption cross 420 sections of 3.8 ± 0.5 and 1.4 ± 0.5 m^2/g , respectively, are capable to cover the short-wavelength variation in σ_{abs}^{nonBC}

¹ https://www.dwd.de/EN/research/observing_atmosphere/composition_atmosphere/aerosol/cont_nav/saharan_dust.html

observed for the UFS snow samples. Here, a reasonable mass concentration of 4 and 18 ng/mL was assumed for the 30 and 50% OC sample, respectively, to calculate the snow mass specific absorption cross section of BrC, σ_{abs}^{BrC} , from the corresponding MAC that is given in Schnaiter et al. (2006). In summary, from a spectroscopic perspective the additional light absorbing particle mass observed in the fresh UFS snow samples can be explained by long-range transported Saharan desert dust and/or BrC particles that are co-deposited in the snow together with the BC particles in varying compositions and mass concentrations.

To further examine the nature of the particulate components that are deposited in the snow samples ion chromatography (IC) and an inductive coupled plasma mass spectrometry (ICP-MS) analysis were exemplarily conducted for the snow sample from March 10, 2017, mainly to clarify the concentration of higher ions which

might be present in the snow. Additionally, the aerosol released from this snow sample was fed to a Waveband Integrated Bioaerosol Sensor (University of Hertfordshire, UK, WIBS4) to get information on the biogenic particle fraction. For these additional analyses, re-aerosolized airborne particles were sampled downstream the nebulizing system behind the dryer by substituting the PAAS-3λ and the SP2 (see Figure 1). A Nuclepore™ filter with pore sizes of 0.2 μ m was taken for Environmental Scanning Electron Microscopy (ESEM; Quattro S, ThermoFisher

Scientific, USA) microscopy combined with EDX microanalysis (EDAX, Octane Elite Super) to further characterize the different particle types found mainly in the larger particle size range (larger than \sim 500 nm) of this sample. The snow sample from March 10, 2017 has a mass concentration $c_{BC}^{SP2}=2.8$ ng/mL and an equivalent BC

mass concentration of $c_{BC}^{equiv}=6.0$ ng/ml for $\lambda=532$ nm, which gives an enhancement factor of $\gamma = 2.1$. Therefore, the March 10 sample represents the bulk of the samples in terms of γ , but is on the lower side concerning c_{BC}^{SP2} and c_{BC}^{equiv} concentrations (see Figure 11). The IC analysis of the snow sample, which was set to detect anions, shows only little concentrations of chloride, nitrate and sulphate of 0.29, 1.1 and 0.3 mg/L, respectively. Only very low concentrations of alkaline and alkaline earth metals were found from the ICP-MS analysis. For the trace metals manganese, iron, copper and zinc concentrations of 9.7 μ g/L, 1.7 μ g/L, 1.1 μ g/L and 8.7 μ g/L were found, respectively.

The ESEM micrographs reveal that the larger (\sim 500 nm) particles extracted from the March 10 snow sample predominantly consist of biogenic and biological materials including fragments of cellular membranes, whole bacteria, pollen, spores, and their mixtures. Mineral dust particles could be identified in the sample too, but to a much less extent than the biogenic particles. Figure 13 gives an overview composite image of a typical Nuclepore™ filter area, where particles with heavier elements like Al, Si, Fe, Mg, K, and Ti, are accentuated in

green color due to their brighter response in the backscatter electron detector (BSED). These elements are typically found in mineral dust particles, as compared to the lighter elements like C, N, O, Na, and S typical for biological material. This overview picture highlights the low relative abundance of mineral dust particles in the coarse mode particle size range of the sample. Representative examples of individual particles are given in Figure 14 Figure 16.

Note that the EDX spectra of all analyzed particles are very characteristic for particle agglomerates or for chemical aging. The biogenic particle (Figure 14) has areas showing intracellular composition (spot A) and pure cellular

membrane fragments (spot B), whereas the mineral dust particle (Figure 15) and soot particle (Figure 16) exhibit spectra characteristics for both inorganic and biogenic material. An example of a Fullerene soot aggregate, emitted from one of the aqueous suspension standards is shown in Figure 17. As expected, the Fullerene soot particle does not contain any foreign chemical elements, as shown by the EDX spectrum in the right panel of Figure 17.

460 The WIBS4 discriminates fluorescing biological aerosol particles (FBAP) by combining single particle fluorescence signals from two excitation/emission wavebands with a low cross-sensitivity to inorganic, combustion, and mineral dust particles (Toprak and Schnaiter, 2013). The WIBS4 measurement of the March 10, 2017 snow sample supports the ESEM results of a high fraction of biogenic particles (43%) in the size range larger than 0.5 μm . The size segregated analysis reveals biogenic particle fractions of 80% and 100% for sizes larger than 465 2 μm and 3 μm , respectively.

While these results give a detailed look into the physical and chemical nature of the particles that might contribute the light absorption in the March 10 snow sample, they cannot be used to draw conclusions for all snow samples. Here, further analyses are required that couldn't be conducted within the scope of this pilot study. However, one question that arises from the above findings is whether the biogenic particles found in the March 10 snow 470 sample can be attributed to BrC, which was shown to be a good candidate for explaining the additional light absorption in the snow samples (Figure 12). The term "brown carbon" is mainly related to a strong wavelength dependence of the visible light absorption observed in these materials. From a chemical perspective, BrC can generally be divided into humic-like substances (HULIS) and tar balls (Wu et al., 2016). HULIS can be characterised mainly as a mixture of macromolecular organic compounds with various functional groups and are 475 expected e.g. in oxidation processes of biogenic precursors (Wu et al., 2016). Tar balls are emitted from biomass burning and are of spherical, amorphous structure and are typically not aggregated. Moreover, light absorbing organic material and HULIS can be formed from the water-soluble fraction of biomass burning aerosol compounds, and is therefore suggested as an atmospheric process for the formation of light absorbing BrC in cloud droplets (Hoffer et al., 2004). Further examination of snow samples from different locations as well as systematic 480 investigations on the optical behaviour of biogenic particulate matter is therefore necessary to evaluate the influence of biogenic (including biological), BrC and mineral dust on the aerosol absorption properties in the visible spectral range.

6. Conclusions

In this study a new laboratory analysis method for snow and ice samples was presented. With this method the snow 485 mass specific absorption cross section σ_{abs} is directly measured by the three-wavelength photoacoustic absorption spectrometer PAAS-3 λ on re-aerosolized snow samples without particle deposition on filters. The refractory black carbon (BC) mass concentration in the snow samples was concurrently determined using a single particle soot photometer (SP2). Using water suspensions of Fullerene soot particles of known BC mass concentrations as a BC reference for the snow samples, the aerosolization efficiency of the nebulizer was quantified and the detection 490 limit of the method was assessed. Further, the mass specific absorption cross section of Fullerene soot (MAC_{FS}) was determined for the visible spectral range from the concurrent PAAS-3 λ and SP2 measurements.

The method was then used to analyse 31 fresh snow samples collected at the Environmental Research Station Schneefernerhaus (UFS) in the winter period 2016/2017. The spectral snow mass specific absorption cross sections σ_{abs} measured by the PAAS-3 λ were analysed as a function of the refractory BC snow mass mixing ratio c_{BC}^{SP2} 495 deduced by the SP2 to determine the BC mass specific absorption cross section (MAC) and the equivalent BC mass mixing ratio c_{BC}^{equiv} of the snow samples. Contrasting the MAC of the snow samples with the MAC_{FS} of the Fullerene soot reference BC material, it was found that the MAC of the snow particles was enhanced by a factor

of two in the blue and green part of the visible spectrum, resulting in an enhanced c_{BC}^{equiv} mass mixing ratio compared to c_{BC}^{SP2} . While the latter accounts only for the refractory BC it was concluded that the discrepancy 500 between the optically deduced c_{BC}^{equiv} and the c_{BC}^{SP2} suggests the presence of light absorbing non-BC particles in the snow samples. The good correlation between c_{BC}^{equiv} and c_{BC}^{SP2} further indicates that the non-BC and BC aerosol particles have either the same source (e.g. biomass burning) or experienced a significant atmospheric processing (internal mixing) before they were deposited into the snow. Using the MAC_{FS} of Fullerene soot and the c_{BC}^{SP2} mass mixing ratio measured for the snow samples, the snow mass specific absorption cross section σ_{abs}^{nonBC} of the non-505 BC particles could be determined. The spectral behaviour of σ_{abs}^{nonBC} gives mean absorption Angström exponents of 2.2 and 1.5 for the 405 to 532 nm and 532 to 658 nm spectral ranges, respectively, indicating that the non-BC light absorbing particle mass is predominantly absorbing in the blue to green part of the visible spectrum and less in the red. By comparing σ_{abs}^{nonBC} with laboratory data for Saharan dust and organic (brown) carbon, it could be shown that these atmospheric aerosol components can explain the observed non-BC light absorption in the snow. 510 Additional analyses of an exemplary snow sample using environmental scanning electron microscopy combined with EDX microanalysis as well as single particle fluorescence measurements revealed that the larger particles of the snow sample are predominantly of biogenic or organic origin with lower contributions from mineral dust. This finding supports the above interpretation that the additional non-BC light absorbing aerosol mass is likely due to biogenic particles, brown carbon, and mineral dust. However, further studies are required including samples from 515 other locations, to quantify the general contribution of these non-BC atmospheric aerosol components to the visible light absorption in snow and ice surfaces and the resulting albedo reduction.

7. Acknowledgements

We thank Ludwig Ries, German Federal Environment Agency (UBA) and Gerhard Müller, German Meteorological Service (DWD), Global Observatory Zugspitze/Hohenpeissenberg for providing weather, 520 atmospheric BC and Saharan dust inventory data. Joshua Schwarz, National Oceanic and Atmospheric Administration (NOAA), Boulder, USA is thanked for providing snow sample data for comparison. This work was funded within the Helmholtz Research Program Atmosphere and Climate.

8. Tables

525 Table 1: Overview of the optical and BC mass properties measured for the Fullerene soot suspension standards as well as the fresh snow samples.

	Fullerene Soot	UFS Snow Samples
MAC (405 nm) [m ² /g] (mean \pm 1 σ) (5 - 95th percentile range)	10.5 \pm 3.2 7.6 - 14.0	21.1 \pm 7.9 13.4, 33.1
MAC (532 nm) [m ² /g] (mean \pm 1 σ) (5 - 95th percentile range)	9.5 \pm 2.2 7.7 - 16.0	18.2 \pm 7.2 10.9, 27.2
MAC (658 nm) [m ² /g] (mean \pm 1 σ) (5 - 95th percentile range)	8.6 \pm 3.3 5.7, 10.9	11.9 \pm 4.6 8.1, 20.2
AAE (405 - 658 nm) AAE (405 - 532 nm) AAE (532 - 658 nm) (mean \pm 1 σ)	0.46 \pm 0.07 0.35 \pm 0.08 0.60 \pm 0.12	1.20 \pm 0.85 0.49 \pm 1.00 2.10 \pm 2.24
Mass Median Diameter [nm] (mean \pm 1 σ) (5 - 95th percentile range)	228 \pm 3 223.5 - 233	207.5 \pm 42.1 146.2 - 290.4
1 σ Distribution Width (mean \pm c) (5 - 95th percentile range)	1.57 \pm 0.018 1.54 - 1.6	1.83 \pm 0.13 1.64 - 2.06
σ_{abs} (405 nm) [10 ⁻⁸ m ² /mL] (median, 5 - 95th percentile range)		9.9, 4.3 - 37.9
σ_{abs} (532 nm) [10 ⁻⁸ m ² /mL] (median, 5 - 95th percentile range)		8.4, 2.9 - 34.2
σ_{abs} (658 nm) [10 ⁻⁸ m ² /mL] (median, 5 - 95th percentile range)		5.9, 1.9 - 21.5
c_{BC}^{SP2} [ng/mL] (median, 5 - 95th percentile range)		5.0, 1.7 - 20.4
c_{BC}^{equi} (532 nm) [ng/mL] (median, 5 - 95th percentile range)		8.9, 3.1 - 36.1

9. Figures

530

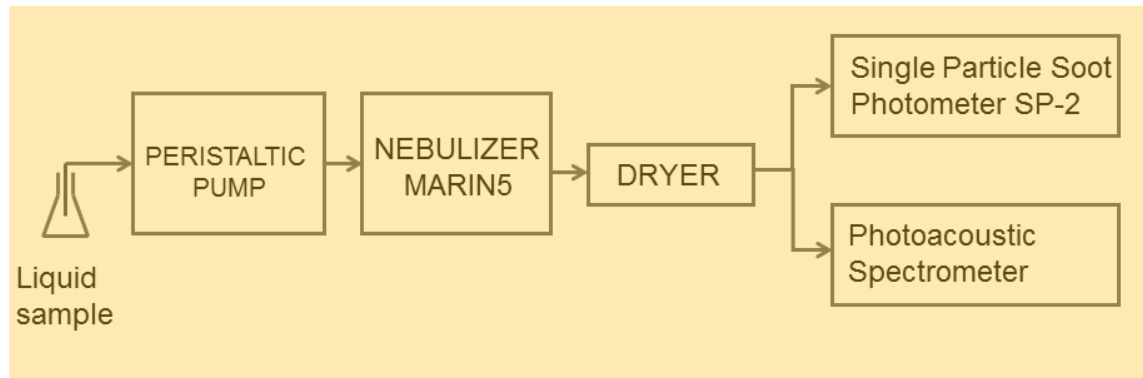


Figure 1: Schematic of the instrumental setup used in the present study.

535

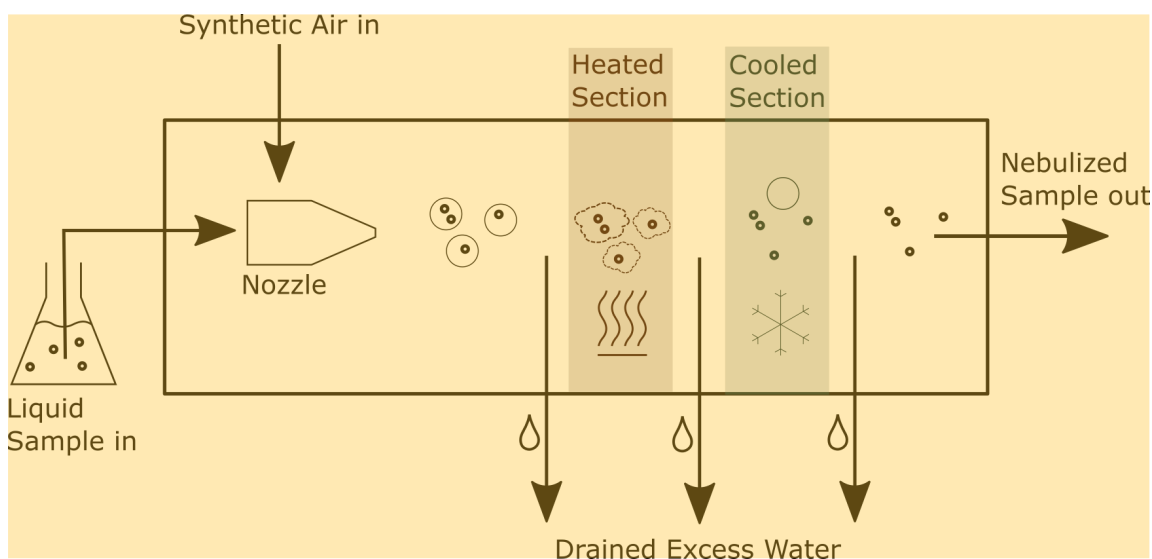


Figure 2: Operation principle of the CETAC Marin-5 nebulizer used in the present study.

540

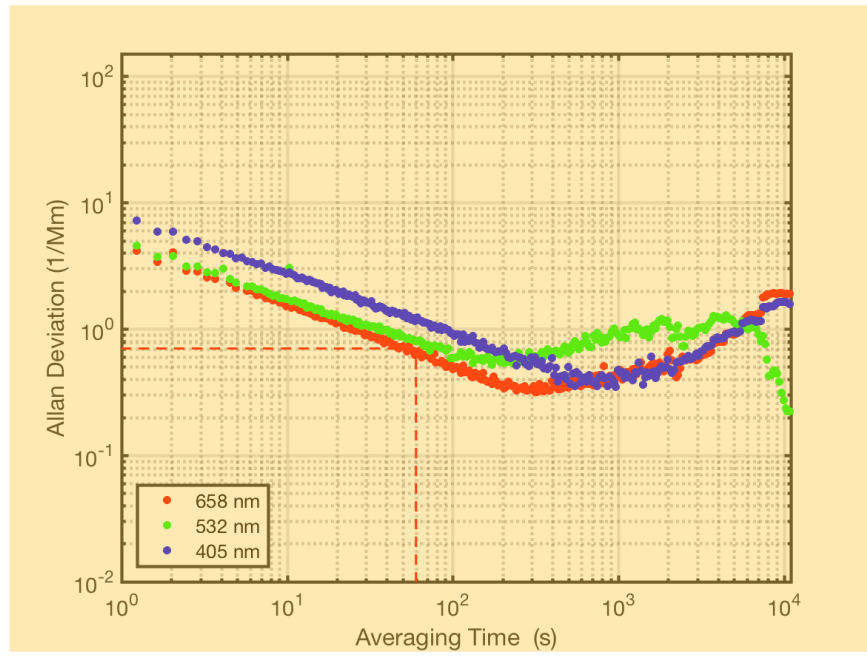


Figure 3: Allan deviation analysis of a long-term photoacoustic background measurement. The red dashed lines indicate the typical averaging time of 60 s used in the PAAS-3 λ measurements and the corresponding Allan deviation (1 σ) of 0.7 1/Mm.

545

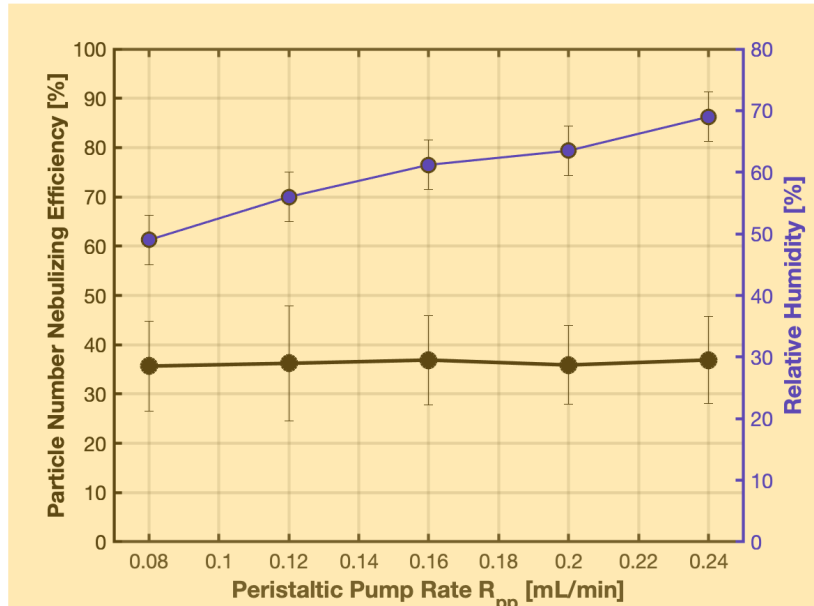
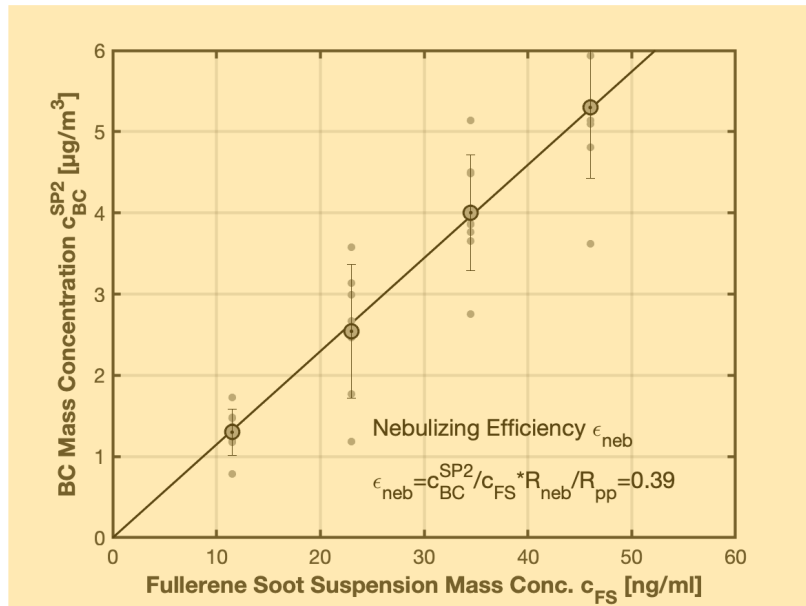


Figure 4: Particle number nebulizing efficiency and relative humidity of the output aerosol flow as a function of the peristaltic pump flow rate applied in Marin-5 nebulizing tests with PSL particle suspensions.



550 Figure 5: Particle mass nebulizing efficiency of the Marin-5 nebulizer using Fullerene soot suspensions with defined BC mass concentrations c_{FS} . The refractory BC mass concentration c_{BC}^{SP2} was measured in the dry aerosol exit flow of the nebulizer using a Single Particle Soot Photometer (SP2). R_{neb} and R_{pp} define the flow rates of the dispersing gas and the liquid sample supply, respectively. See text for details.

555

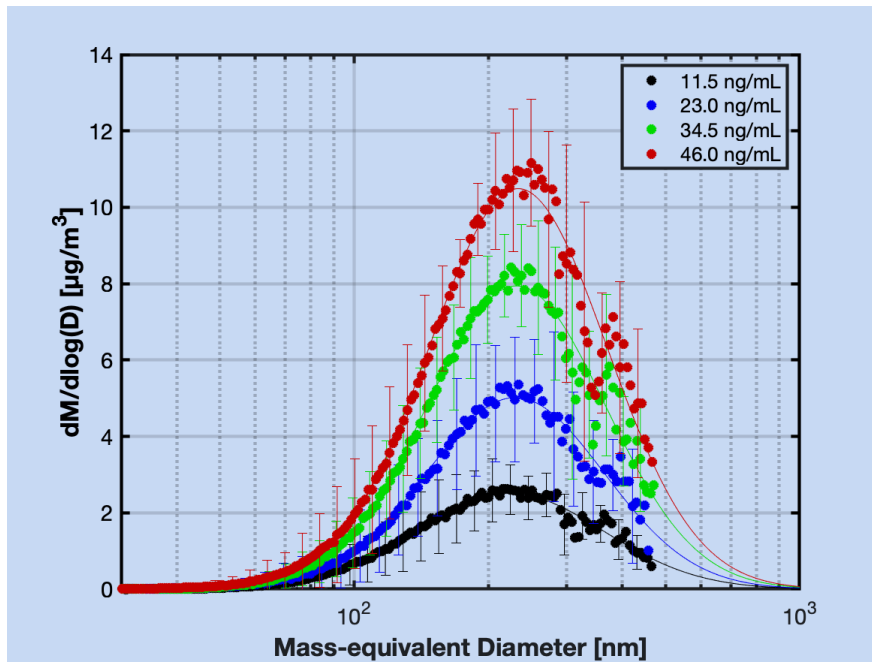
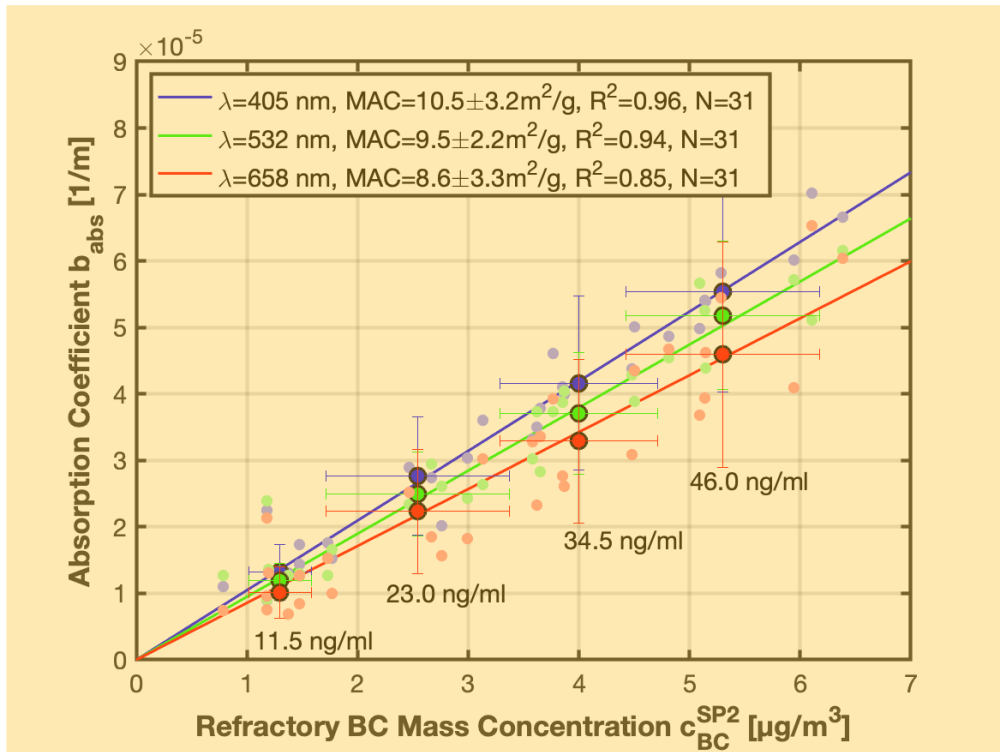


Figure 6: Particle mass size distributions of the Fullerene soot suspensions used to characterize the Marin-5 nebulizer. The measurements were conducted with the SP2, which has an upper size limit of 560 nm in the present study. Results from lognormal fits are represented by the thin lines.



560

Figure 7: Determination of the mass specific absorption cross section (MAC) of re-aerosolized Fullerene soot suspension standards at 405, 532, and 658 nm. The MAC values are given in the legend and are derived from concurrent measurements of the absorption coefficient, b_{abs} , using the photoacoustic aerosol absorption spectrometer PAAS-3λ and the refractory BC mass concentration, c_{BC}^{SP2} , using the SP2.

565

570

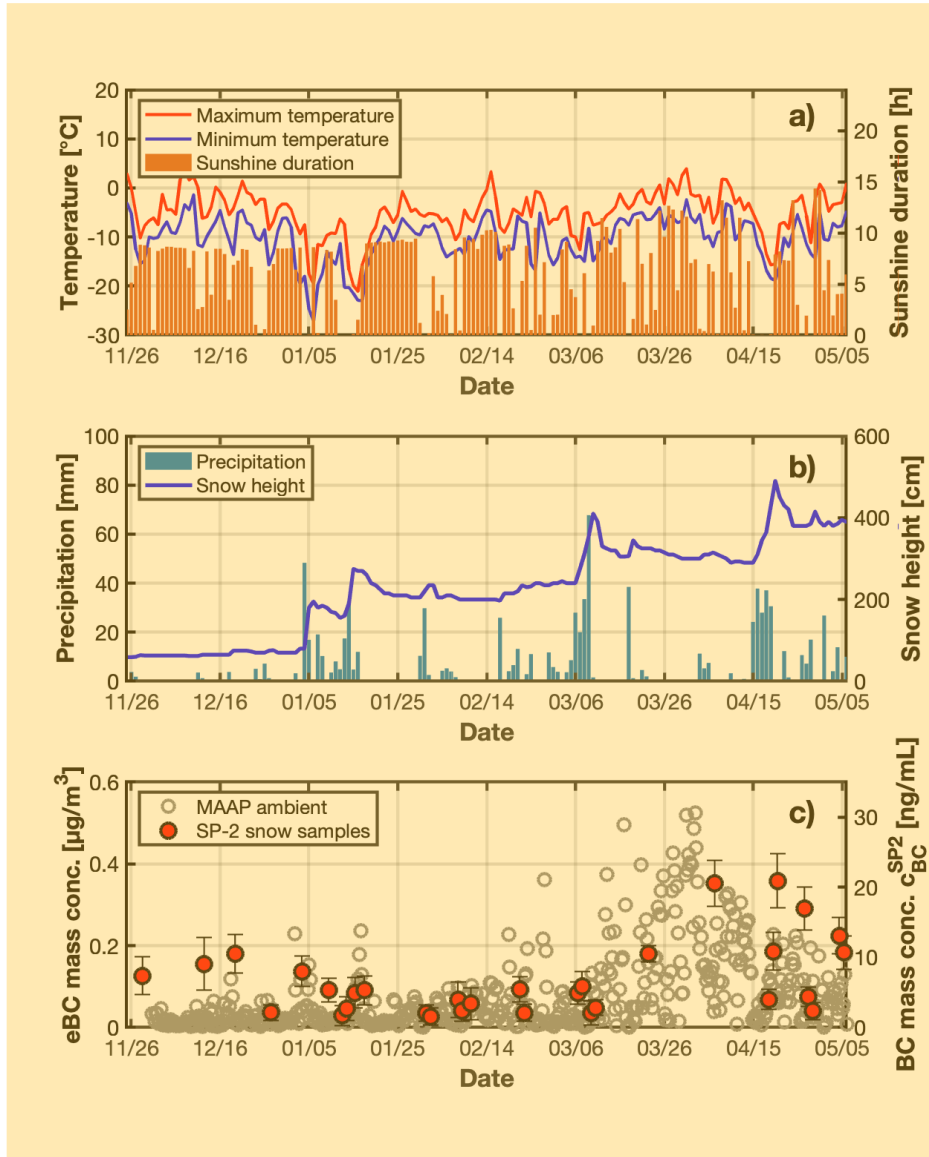
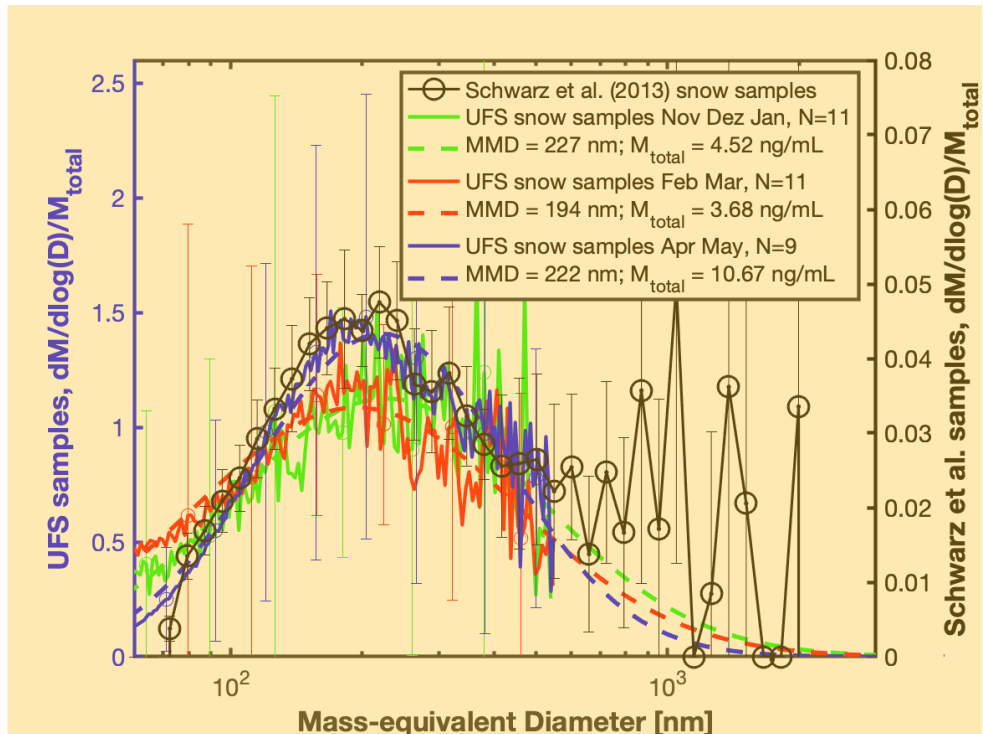


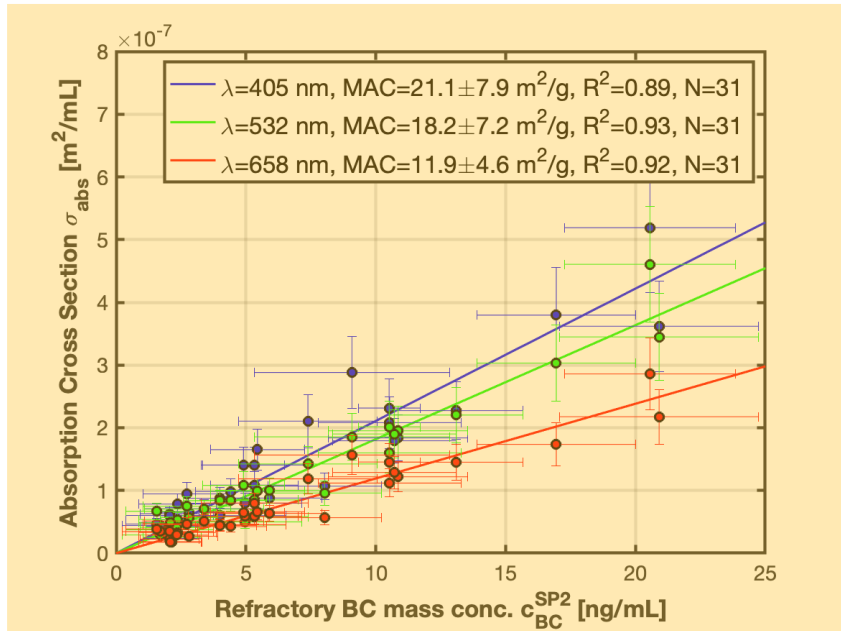
Figure 8: Overview of the meteorological and ambient BC conditions during the period the snow samples were collected at UFS. The data in (a) to (b) are on a daily basis. The atmospheric equivalent black carbon (eBC) mass concentrations shown in panel (c) represent 30 min averages of the MAAP measurements. Note that the refractory black carbon mass concentrations, c_{BC}^{SP2} , deduced from the SP2 measurements of the re-aerosolized snow samples are compared in panel (c) with the atmospheric eBC mass concentration. See text for details concerning data providers, sampling, and measurement methods.



580

Figure 9: BC mass size distributions of the snow samples deduced from the SP2 measurements. The size distributions are averaged over the three periods Nov-Dec-Jan (green), Feb-Mar (red), and Apr-May (blue) and are normalized by the total mass (M_{total}). Lognormal fits are represented by the dashed lines. Fit results in terms of mass median diameter (MMD) and integrated mass (M_{total}) are given in the legend. An averaged size distribution for fresh snow samples published by Schwarz et al. (2013) is shown for comparison (black line and open circles)

585



590

Figure 10: Snow mass specific absorption cross section σ_{abs} of the snow samples (Eq. 1) as a function of the mass concentration $c_{\text{BC}}^{\text{SP2}}$ deduced from the SP2 measurements. The BC mass specific absorption cross section, MAC, is deduced from a linear regression fit of the data per wavelength and is given in the legend. See text for details.

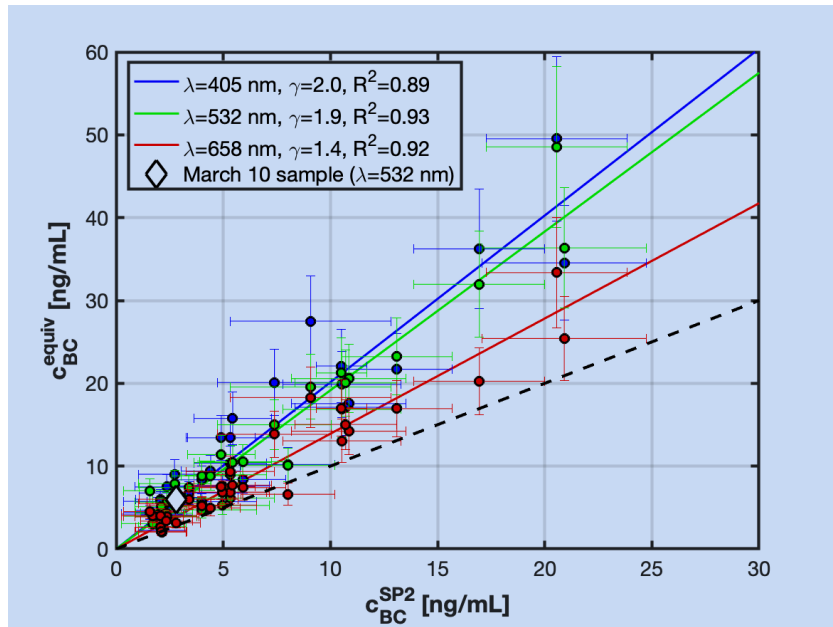


Figure 11: Equivalent BC mass concentration c_{BC}^{equiv} , Eq. (2), of the snow samples as a function of the refractory BC mass concentration c_{BC}^{SP2} . The dashed black line represents the 1:1 line. Linear regression fits per wavelength gives the mass “enhancement” factor γ , which is given in the legend. The white diamond symbol marks the 532 nm values of the March 10 snow sample that was further analyzed for elemental composition, particle morphology, and fluorescence response. See text for details.

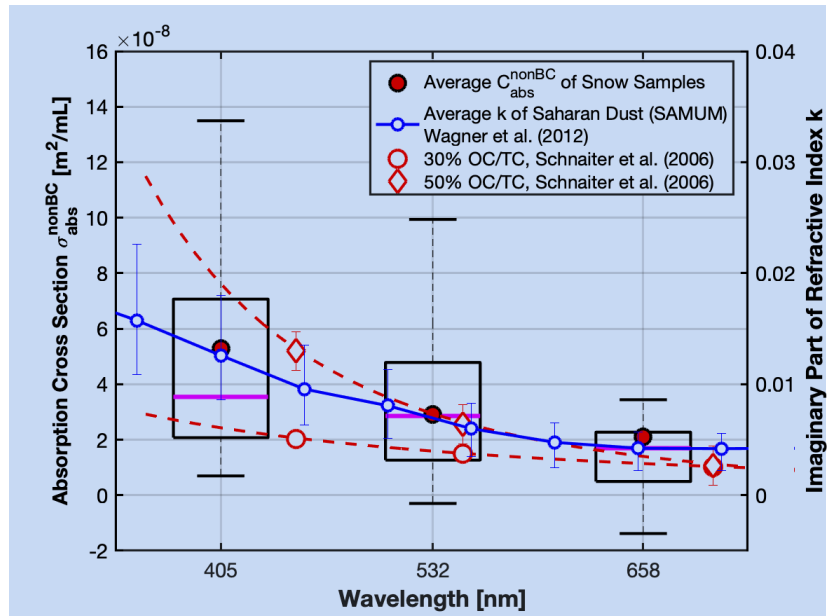
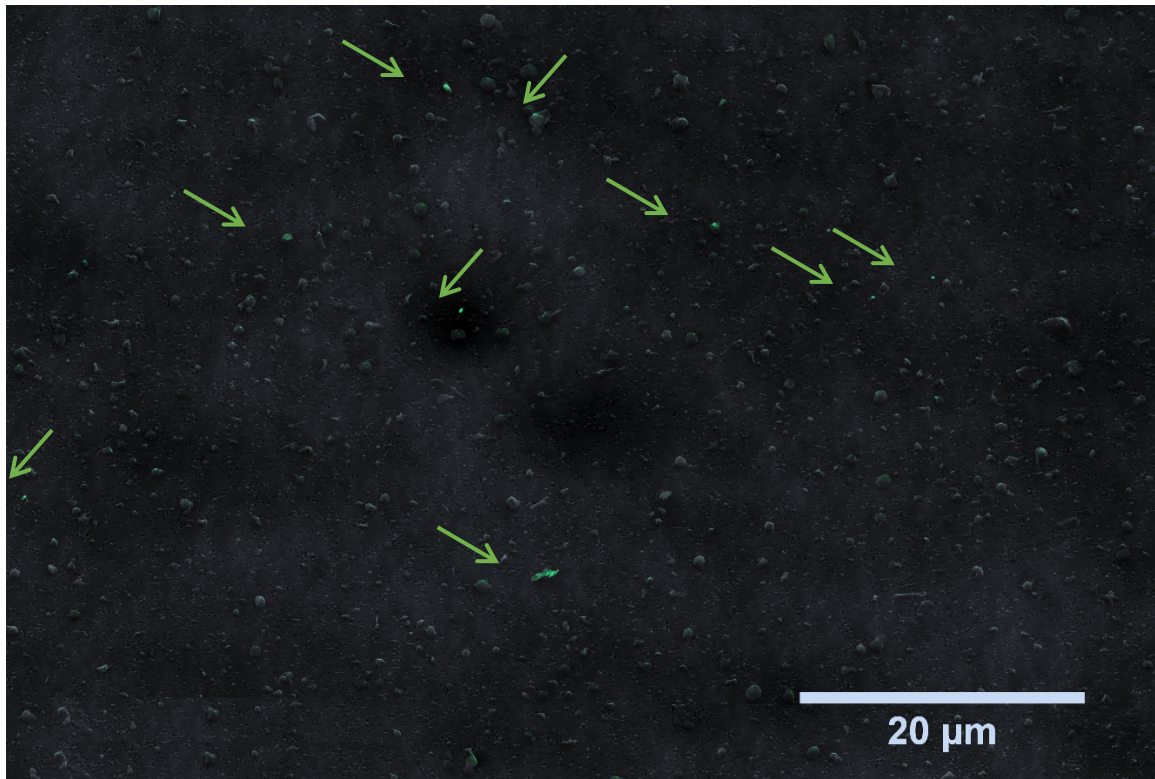
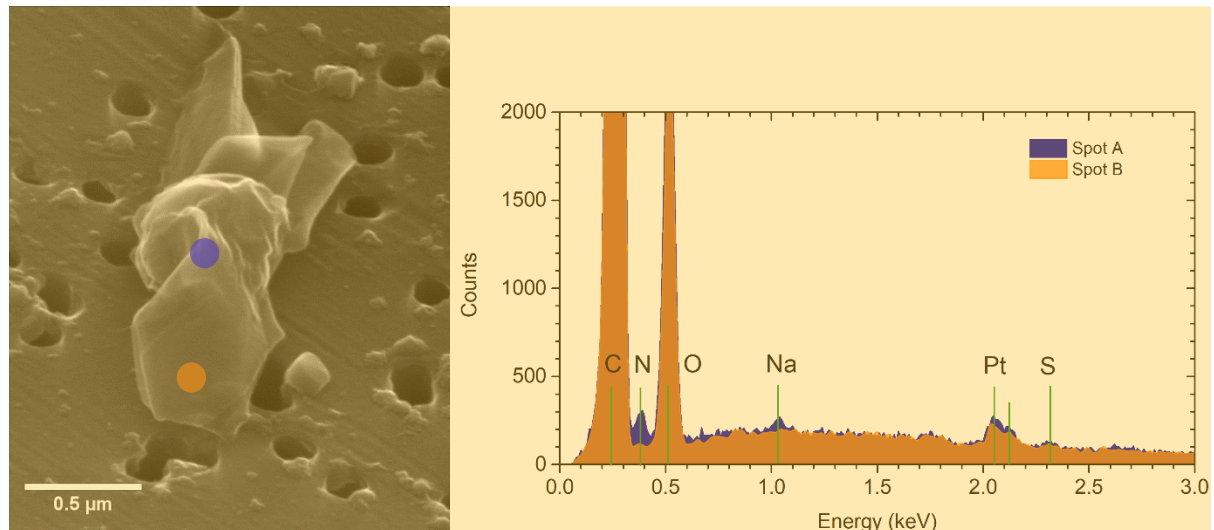


Figure 12: Statistical analysis of the snow mass specific absorption cross section σ_{abs}^{nonBC} of the non-BC particles deduced from Eq. (3). Laboratory data for Saharan dust (blue) and brown carbon (red) are shown for comparison. Two examples of brown carbon (BrC) with organic to total carbon mass ratio, OC/TC, of 30% and 50% are selected to emphasize the possible variability in spectral absorption of this class of atmospheric aerosol mass. A BrC in snow mass concentration of 4 and 18 ng/mL was assumed for the 30 and 50% example, respectively.



610 Figure 13: Overview of residual particles extracted from a snow sample via Marin-5. The image is a false color overlay from secondary electron (SE) detector (black and white image) and backscatter electron detector, BSED (the green spots). The particles containing elements with higher atomic number are visible as green spots and are highlighted by green arrows.



615 Figure 14: Morphology and composition of biological residual particle extracted from snow sample behind Marin-5 on a Nuclepore™ filter. Left panel: the SEM secondary electron image. Right panel: EDX-spectrum obtained from different areas of the particle (marked as color spots in the image). A clear biogenic signature (N, S, Na) is visible for the central bulky part suggesting intracellular composition (spot A, blue color), whereas the exterior part of the particle shows pure carbonaceous compounds (C, O) (spot B, orange color). Sample coating is responsible for the platinum peak.

620

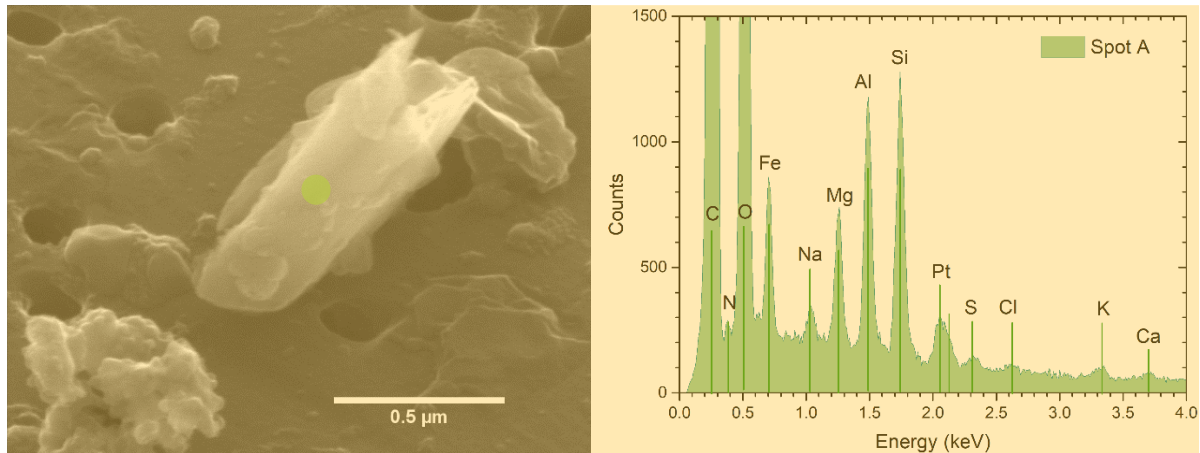


Figure 15: Same as Fig. 14 but for a mineral dust particle. The EDX-spectrum of the particle identifies chemical patterns that are characteristic for mineral dust (Al, Si, Mg, Fe, K, Ca), biogenic (N, Na, Cl, S), and carbonaceous (C, O) materials.

625

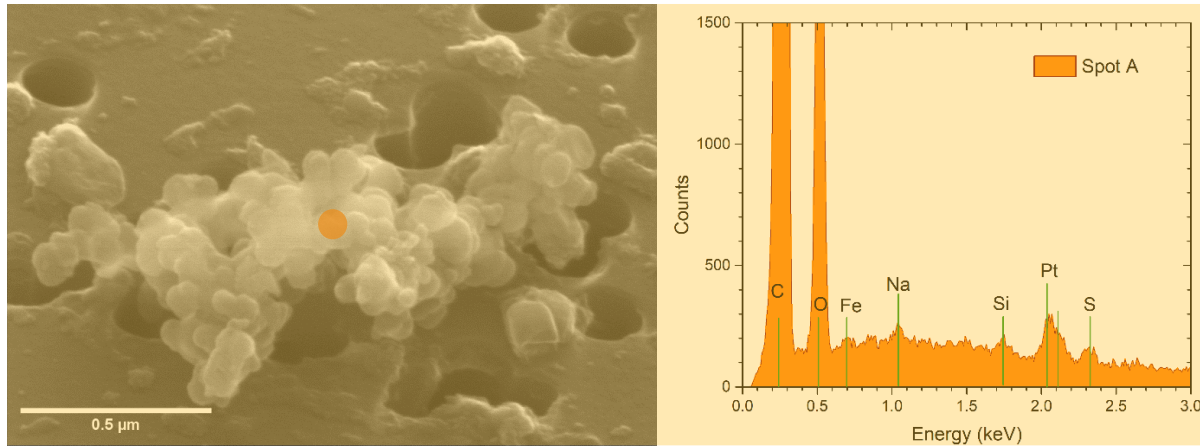


Figure 16: Same as Fig. 14 but for a soot (BC) particle. The EDX-spectrum of the particle reveals trace elements of Fe, Na, Si, and S in addition to the dominating C, O pattern that is characteristic for carbonaceous matter.

630

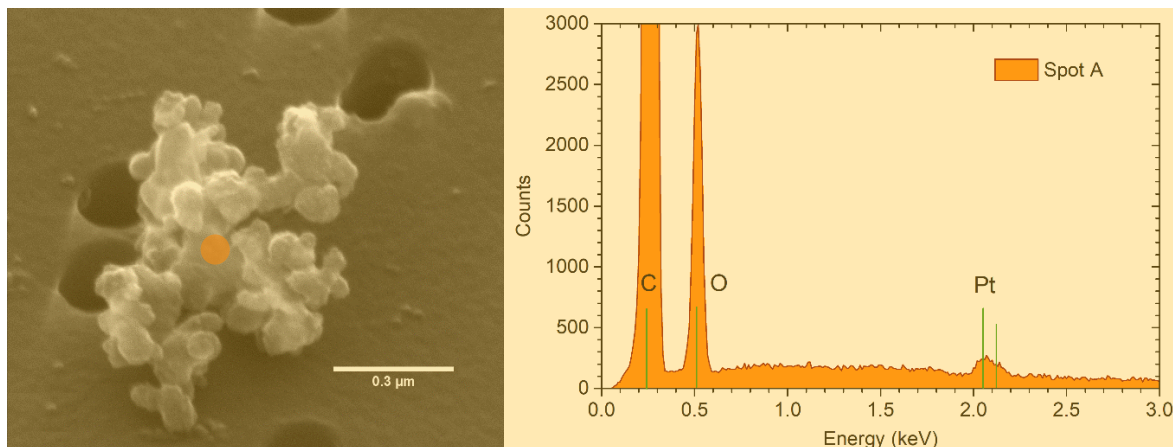


Figure 17: Same as Fig. 14 but for a Fullerene soot particle from the particle standard suspensions. The EDX-spectrum of the particle collected from the spot A shows a pure carbonaceous signature with only the C and O peaks. Sample coating is responsible for the Pt peak at 2.08 keV.

635

References

Baumgardner, D., Popovicheva, O., Allan, J., Bernardoni, V., Cao, J., Cavalli, F., Cozic, J., Diapouli, E., Eleftheriadis, K., Genberg, P. J., Gonzalez, C., Gysel, M., John, A., Kirchstetter, T. W., Kuhlbusch, T. A. J., Laborde, M., Lack, D., Müller, T., Niessner, R., Petzold, A., Piazzalunga, A., Putaud, J. P., Schwarz, J., Sheridan, P., Subramanian, R., Swietlicki, E., Valli, G., Vecchi, R. and Viana, M.: Soot reference materials for instrument calibration and intercomparisons: A workshop summary with recommendations, *Atmos. Meas. Tech.*, 5(8), 1869–1887, doi:10.5194/amt-5-1869-2012, 2012.

Birmili, W., Göbel, T., Sonntag, A., Ries, L., Sohmer, R., Gilge, S., Levin, I. and Stohl, A.: A case of transatlantic aerosol transport detected at the Schneefernerhaus observatory (2650m) on the northern edge of the Alps, *Meteorol. Zeitschrift*, 19(6), 591–600, doi:10.1127/0941-2948/2010/0465, 2010.

Bond, T. C., Doherty, S. J., Fahey, D. W., Forster, P. M., Berntsen, T., Deangelo, B. J., Flanner, M. G., Ghan, S., Kärcher, B., Koch, D., Kinne, S., Kondo, Y., Quinn, P. K., Sarofim, M. C., Schultz, M. G., Schulz, M., Venkataraman, C., Zhang, H., Zhang, S., Bellouin, N., Guttikunda, S. K., Hopke, P. K., Jacobson, M. Z., Kaiser, J. W., Klimont, Z., Lohmann, U., Schwarz, J. P., Shindell, D., Storelvmo, T., Warren, S. G. and Zender, C. S.: Bounding the role of black carbon in the climate system: A scientific assessment, *J. Geophys. Res. Atmos.*, 118(11), 5380–5552, doi:10.1002/jgrd.50171, 2013.

Boucher, O., Randall, D., Artaxo, P., Bretherton, C., Feingold, G., Forster, P., Kärmenen, V.-M. V.-M., Kondo, Y., Liao, H., Lohmann, U., Rasch, P., Satheesh, S. K., Sherwood, S., Stevens, B., Zhang, X. Y. and Zhan, X. Y.: Clouds and Aerosols, *Clim. Chang. 2013 Phys. Sci. Basis. Contrib. Work. Gr. I to Fifth Assess. Rep. Intergov. Panel Clim. Chang.*, 571–657, doi:10.1017/CBO9781107415324.016, 2013.

Clarke, A. D. and Noone, K. J.: Soot in the Arctic snowpack: a cause for perturbations in radiative transfer, *Atmos. Environ.*, 19(12), 2045–2053, doi:10.1016/0004-6981(85)90113-1, 1985.

Dal Farra, A., KASPAKI, S., BEACH, J., BUCHELI, T. D., SCHAEPMAN, M. and SCHWIKOWSKI, M.: Spectral signatures of submicron scale light-absorbing impurities in snow and ice using hyperspectral microscopy, *J. Glaciol.*, 64(245), 377–386, doi:10.1017/jog.2018.29, 2018.

Doherty, S. J., Warren, S. G., Grenfell, T. C., Clarke, A. D. and Brandt, R. E.: Light-absorbing impurities in Arctic snow, *Atmos. Chem. Phys.*, 10(23), 11647–11680, doi:10.5194/acp-10-11647-2010, 2010.

Dong, Z., Kang, S., Qin, D., Shao, Y., Ulbrich, S. and Qin, X.: Variability in individual particle structure and mixing states between the glacier-snowpack and atmosphere in the northeastern Tibetan Plateau, *Cryosphere*, 12(12), 3877–3890, doi:10.5194/tc-12-3877-2018, 2018.

Fischer, D. Al and Smith, G. D.: A portable, four-wavelength, single-cell photoacoustic spectrometer for ambient aerosol absorption, *Aerosol Sci. Technol.*, 52(4), 393–406, doi:10.1080/02786826.2017.1413231, 2018.

Flanner, M. G., Zender, C. S., Randerson, J. T. and Rasch, P. J.: Present-day climate forcing and response from black carbon in snow, *J. Geophys. Res. Atmos.*, 112(11), 1–17, doi:10.1029/2006JD008003, 2007.

Flentje, H., Briel, B., Beck, C., Collaud Coen, M., Fricke, M., Cyrys, J., Gu, J., Pitz, M. and Thomas, W.: Identification and monitoring of Saharan dust: An inventory representative for south Germany since 1997, *Atmos. Environ.*, 109, 87–96, doi:10.1016/j.atmosenv.2015.02.023, 2015.

Gilge, S., Plass-Duelmer, C., Fricke, W., Kaiser, A., Ries, L., Buchmann, B. and Steinbacher, M.: Ozone, carbon monoxide and nitrogen oxides time series at four alpine GAW mountain stations in central Europe, *Atmos. Chem. Phys.*, 10(24), 12295–12316, doi:10.5194/acp-10-12295-2010, 2010.

Gorelik, O. P., Dyuzhev, G. A., Novikov, D. V., Oichenko, V. M. and Fursei, G. N.: Cluster structure of fullerene-containing soot and C60 fullerene powder, *Tech. Phys.*, 45(11), 1489–1495, doi:10.1134/1.1325035, 2002.

Grenfell, T. C., Doherty, S. J., Clarke, A. D. and Warren, S. G.: Light absorption from particulate impurities in snow and ice determined by spectrophotometric analysis of filters, *Appl. Opt.*, 50(14), 2037, doi:10.1364/ao.50.002037, 2011.

Gysel, M., Laborde, M., Olfert, J. S., Subramanian, R. and Gréhn, A. J.: Effective density of Aquadag and fullerene soot black carbon reference materials used for SP2 calibration, *Atmos. Meas. Tech.*, 4(12), 2851–2858,

doi:10.5194/amt-4-2851-2011, 2011.

685 Heintzenberg, J.: The SAMUM-1 experiment over Southern Morocco: Overview and introduction, *Tellus, Ser. B Chem. Phys. Meteorol.*, 61(1), 2–11, doi:10.1111/j.1600-0889.2008.00403.x, 2009.

Hoffer, A., Kiss, G., Blaszó, M. and Gelencsér, A.: Chemical characterization of humic-like substances (HULIS) formed from a lignin-type precursor in model cloud water, *Geophys. Res. Lett.*, 31(6), n/a-n/a, doi:10.1029/2003gl018962, 2004.

690 Kahnert, M., Nousiainen, T., Lindqvist, H. and Ebert, M.: Optical properties of light absorbing carbon aggregates mixed with sulfate: assessment of different model geometries for climate forcing calculations, *Opt. Express*, 20(9), 10042, doi:10.1364/oe.20.010042, 2012.

Kaspari, S., Painter, T. H., Gysel, M., Skiles, S. M. and Schwikowski, M.: Seasonal and elevational variations of black carbon and dust in snow and ice in the Solu-Khumbu, Nepal and estimated radiative forcings, *Atmos. Chem. Phys.*, 14(15), 8089–8103, doi:10.5194/acp-14-8089-2014, 2014.

695 Kaspari, S. D., Schwikowski, M., Gysel, M., Flanner, M. G., Kang, S., Hou, S. and Mayewski, P. A.: Recent increase in black carbon concentrations from a Mt. Everest ice core spanning 1860–2000 AD, *Geophys. Res. Lett.*, 38(4), doi:10.1029/2010GL046096, 2011.

Katich, J. M., Perring, A. E., Schwarz, J. P. and Wang, J.: Aerosol Science and Technology Optimized detection 700 of particulates from liquid samples in the aerosol phase: Focus on black carbon Optimized detection of particulates from liquid samples in the aerosol phase: Focus on black carbon, , doi:10.1080/02786826.2017.1280597, 2017.

Kondo, Y., Sahu, L., Moteki, N., Khan, F., Takegawa, N., Liu, X., Koike, M. and Miyakawa, T.: Consistency 705 and traceability of black carbon measurements made by laser-induced incandescence, thermal-optical transmittance, and filter-based photo-absorption techniques, *Aerosol Sci. Technol.*, 45(2), 295–312, doi:10.1080/02786826.2010.533215, 2011.

Laborde, M., Mertes, P., Zieger, P., Dommen, J., Baltensperger, U. and Gysel, M.: Sensitivity of the Single 710 Particle Soot Photometer to different black carbon types, *Atmos. Meas. Tech.*, 5(5), 1031–1043, doi:10.5194/amt-5-1031-2012, 2012a.

Laborde, M., Schnaiter, M., Linke, C., Saathoff, H., Naumann, K.-H., Moehler, O., Berlenz, S., Wagner, U., Taylor, J. W., Liu, D., Flynn, M., Allan, J. D., Coe, H., Heimerl, K., Dahlkoetter, F., Weinzierl, B., Wollny, A. G., Zanatta, M., Cozic, J., Laj, P., Hitzenberger, R., Schwarz, J. P. and Gysel, M.: Single Particle Soot Photometer intercomparison at the AIDA chamber, *Atmos. Meas. Tech.*, 5(12), 3077–3097, 2012b.

715 Langridge, J. M., Richardson, M. S., Lack, D. A., Brock, C. A. and Murphy, D. M.: Limitations of the Photoacoustic Technique for Aerosol Absorption Measurement at High Relative Humidity, *Aerosol Sci. Technol.*, 47(11), doi:10.1080/02786826.2013.827324, 2013.

Liu, C., Xu, X., Yin, Y., Schnaiter, M. and Yung, Y. L.: Black carbon aggregates: A database for optical properties, *J. Quant. Spectrosc. Radiat. Transf.*, 222–223, 170–179, doi:10.1016/j.jqsrt.2018.10.021, 2019.

720 Moosmüller, H., Chakrabarty, R. K. and Arnott, W. P.: Aerosol light absorption and its measurement: A review, *J. Quant. Spectrosc. Radiat. Transf.*, 110(11), 844–878, doi:10.1016/j.jqsrt.2009.02.035, 2009.

Schmale, J., Flanner, M., Kang, S., Sprenger, M., Zhang, Q., Guo, J., Li, Y., Schwikowski, M. and Farinotti, D.: Modulation of snow reflectance and snowmelt from Central Asian glaciers by anthropogenic black carbon, *Sci. Rep.*, 7(December 2016), 1–10, doi:10.1038/srep40501, 2017.

725 Schnaiter, M., Linke, C., Möhler, O., Naumann, K. H., Saathoff, H., Wagner, R., Schurath, U. and Wehner, B.: Absorption amplification of black carbon internally mixed with secondary organic aerosol, *J. Geophys. Res.*, doi:10.1029/2005JD006046, 2005.

Schnaiter, M., Gimmler, M., Llamas, I., Linke, C., Jaeger, C. and Mutschke, H.: Strong spectral dependence of light absorption by organic carbon particles formed by propane combustion, *Atmos. Chem. Phys.*, 6, 2981–2990, 2006.

730 Schwarz, J. P., Doherty, S. J., Li, F., Ruggiero, S. T., Tanner, C. E., Perring, A. E., Gao, R. S. and Fahey, D. W.: Assessing Single Particle Soot Photometer and Integrating Sphere/Integrating Sandwich Spectrophotometer

measurement techniques for quantifying black carbon concentration in snow, *Atmos. Meas. Tech.*, 5(11), 2581–2592, doi:10.5194/amt-5-2581-2012, 2012.

735 Schwarz, J. P., Gao, R. S., Perring, A. E., Spackman, J. R. and Fahey, D. W.: Black carbon aerosol size in snow., *Nat. Sci. reports*, 3, 1356, doi:10.1038/srep01356, 2013.

Sinha, P. R., Kondo, Y., Goto-Azuma, K., Tsukagawa, Y., Fukuda, K., Koike, M., Ohata, S., Moteki, N., Mori, T., Oshima, N., Førland, E. J., Irwin, M., Gallet, J. C. and Pedersen, C. A.: Seasonal Progression of the Deposition of Black Carbon by Snowfall at Ny-Ålesund, Spitsbergen, *J. Geophys. Res. Atmos.*, 123(2), 997–1016, doi:10.1002/2017JD028027, 2018.

740 Sun, J., Birmili, W., Hermann, M., Tuch, T., Weinhold, K., Spindler, G., Schladitz, A., Bastian, S., Löschau, G., Cyrys, J., Gu, J., Flentje, H., Briel, B., Asbach, C., Kaminski, H., Ries, L., Sohmer, R., Gerwig, H., Wirtz, K., Meinhardt, F., Schwerin, A., Bath, O., Ma, N. and Wiedensohler, A.: Variability of black carbon mass concentrations, sub-micrometer particle number concentrations and size distributions: results of the German Ultrafine Aerosol Network ranging from city street to High Alpine locations, *Atmos. Environ.*, 202(December 2018), 256–268, doi:10.1016/j.atmosenv.2018.12.029, 2019.

Teng, S., Liu, C., Schnaiter, M., Chakrabarty, R. K. and Liu, F.: Accounting for the effects of nonideal minor structures on the optical properties of black carbon aerosols, *Atmos. Chem. Phys.*, 19(5), 2917–2931, doi:10.5194/acp-19-2917-2019, 2019.

750 Toprak, E. and Schnaiter, M.: Fluorescent biological aerosol particles measured with the Waveband Integrated Bioaerosol Sensor WIBS-4: laboratory tests combined with a one year field study, *Atmos. Chem. Phys.*, 13(1), 225–243, 2013.

Wagner, R., Ajtai, T., Kandler, K., Lieke, K., Linke, C., Mueller, T., Schnaiter, M. and Vragel, M.: Complex refractive indices of Saharan dust samples at visible and near UV wavelengths: a laboratory study, *Atmos. Chem. Phys.*, 12(5), 2491–2512, 2012.

755 Warren G Stephen: optical properties of snow by Warren 1982.pdf, *Rev. Geophys. Sp. Phys.*, 20(1), 67–89, 1982.

Warren, S. G.: Light-Absorbing Impurities in Snow: A Personal and Historical Account, *Front. Earth Sci.*, 6(January 1978), 1–8, doi:10.3389/feart.2018.00250, 2019.

760 Warren, S. G. and Wiscombe, W. J.: A Model for the Spectral Albedo of Snow. II: Snow Containing Atmospheric Aerosols, *J. Atmos. Sci.*, 37, 2734–2745, 1980.

Warren, S. G. and Wiscombe, W. J.: Dirty snow after nuclear war, *Nature*, 313(6002), 467–470, doi:10.1038/313467a0, 1985.

765 Wendl, I. a., Menking, J. a., Färber, R., Gysel, M., Kaspari, S. D., Laborde, M. J. G. and Schwikowski, M.: Optimized method for black carbon analysis in ice and snow using the Single Particle Soot Photometer, *Atmos. Meas. Tech.*, 7(8), 2667–2681, doi:10.5194/amt-7-2667-2014, 2014.

Wu, G. M., Cong, Z. Y., Kang, S. C., Kawamura, K., Fu, P. Q., Zhang, Y. L., Wan, X., Gao, S. P. and Liu, B.: Brown carbon in the cryosphere: Current knowledge and perspective, *Adv. Clim. Chang. Res.*, 7(1–2), 82–89, doi:10.1016/j.accre.2016.06.002, 2016.

770 You, R., Radney, J. G., Zachariah, M. R. and Zangmeister, C. D.: Measured Wavelength-Dependent Absorption Enhancement of Internally Mixed Black Carbon with Absorbing and Nonabsorbing Materials, *Environ. Sci. Technol.*, 50(15), 7982–7990, doi:10.1021/acs.est.6b01473, 2016.

Yuan, Y., Ries, L., Petermeier, H., Trickl, T., Leuchner, M., Couret, C., Sohmer, R., Meinhardt, F. and Menzel, A.: On the diurnal, weekly, and seasonal cycles and annual trends in atmospheric CO₂ at Mount Zugspitze, Germany, during 1981–2016, *Atmos. Chem. Phys.*, 19(2), 999–1012, doi:10.5194/acp-19-999-2019, 2019.

775 Zangmeister, C. D., You, R., Lunny, E. M., Jacobson, A. E., Okumura, M., Zachariah, M. R. and Radney, J. G.: Measured in-situ mass absorption spectra for nine forms of highly-absorbing carbonaceous aerosol, *Carbon N. Y.*, 136, 85–93, doi:https://doi.org/10.1016/j.carbon.2018.04.057, 2018.

Zhang, Y., Kang, S., Li, C., Gao, T., Cong, Z., Sprenger, M., Liu, Y., Li, X., Guo, J., Sillanpää, M., Wang, K., Chen, J., Li, Y. and Sun, S.: Characteristics of black carbon in snow from Laohugou No. 12 glacier on the

780 northern Tibetan Plateau, *Sci. Total Environ.*, 607–608(12), 1237–1249, doi:10.1016/j.scitotenv.2017.07.100, 2017.

Zhang, Y., Kang, S., Sprenger, M., Cong, Z., Gao, T., Li, C., Tao, S., Li, X., Zhong, X., Xu, M., Meng, W., Neupane, B., Qin, X. and Sillanpää, M.: Black carbon and mineral dust in snow cover on the Tibetan Plateau, *Cryosph.*, 12(2), 413–431, doi:10.5194/tc-12-413-2018, 2018.

785 Zhou, Y., Wang, X., Wu, X., Cong, Z., Wu, G. and Ji, M.: Quantifying light absorption of iron oxides and carbonaceous aerosol in seasonal snow across Northern China, *Atmosphere (Basel)*, 8(4), 15–22, doi:10.3390/atmos8040063, 2017.

790